Spin-orbit effects in $Na_4Ir_3O_8$: A hyper-kagome lattice antiferromagnet

Gang Chen

Department of Physics, University of California, Santa Barbara, California 93106-9530, USA

Leon Balents

Kavli Institute for Theoretical Physics, University of California, Santa Barbara, California 93106, USA

(Received 10 June 2008; revised manuscript received 25 July 2008; published 5 September 2008)

We consider spin-orbit coupling effects in $Na_4Ir_3O_8$, a material in which Ir^{4+} spins form an hyper-kagome lattice, a three-dimensional network of corner-sharing triangles. We argue that both low-temperature thermodynamic measurements and the impurity susceptibility induced by dilute substitution of Ti for Ir are suggestive of significant spin-orbit effects. Because of uncertainties in the crystal-field parameters, we consider two limits in which the spin-orbit coupling is either weak or strong compared to the noncubic atomic splittings. A semi-microscopic calculation of the exchange Hamiltonian confirms that indeed large antisymmetric Dzyaloshinskii-Moriya (DM) and/or symmetric exchange anisotropy may be present. In the strong spin-orbit limit, the Ir-O-Ir superexchange contribution consists of *unfrustrated* strong symmetric exchange anisotropy, and we suggest that spin-liquid behavior is unlikely. In the weak spin-orbit limit, and for strong spin-orbit and direct Ir-Ir exchange, the Hamiltonian consists of Heisenberg and DM interactions. The DM coupling is parametrized by a three-component DM vector (which must be determined empirically). For a range of orientation of this vector, frustration is relieved and an ordered state occurs. For other orientations, even the classical ground states are very complex. We perform spin-wave and exact diagonalization calculations, which suggest the persistence of a quantum spin liquid in the latter regime. Applications to $Na_4Ir_3O_8$ and broader implications are discussed.

I. INTRODUCTION

Geometrically frustrated antiferromagnetism is a rich subject enjoying considerable theoretical and experimental attention over several decades of research.[1,2] Such systems are realized by materials containing magnetic ions in which the strongest antiferromagnetic exchanges occur on a network of bonds containing many triangular units. The most celebrated examples are the two-dimensional kagome (corner-sharing triangles) lattice and three-dimensional pyrochlore (corner-sharing tetrahedron) lattice. In ideal classical models, these lattices support highly degenerate ground states, which prevent order down to very low temperature. Instead, the spins continue to fluctuate strongly despite significant correlations induced by the frustrated interactions. Systems in this regime are dubbed (classical) spin liquids or cooperative paramagnets. A major goal in the field is to ascertain whether such spin liquids might also occur even in the zero-temperature limit, in which both quantum effects and many nonideal features of the materials must be taken into account. The answer to this question is quite subtle due to many competing effects that can come into play. Quantum and thermal fluctuations may break the ground-state degeneracy and actually induce magnetic order, an effect known as order by disorder.[3–6] This effect, however, is understood theoretically only in the large spin ($S \gg 1$) limit, in which spins behave semiclassically. Nevertheless, some models even with the smallest possible spins, $S = 1/2$, seem at least qualitatively to follow the order-by-disorder scenario. Conversely, in other models with small spin, quantum spin liquids have been shown to occur. No general theory to predict which of these two tendencies occurs exists at present.

Despite this lack of theoretical discrimination, experimentalists have forged onward in recent years, uncovering a number of promising candidate quantum spin liquid materials with small spin $S = 1/2$ on geometrically frustrated lattices. These include an organic magnet, $\kappa\text{-}(ET)_2Cu_2(CN)_3$, containing spin-1/2 moments on a slightly spatially anisotropic triangular lattice $ZnCu_3(OH)_6Cl_2$, an inorganic realization of a spatially isotropic spin-1/2 kagome antiferromagnet, and very recently the cubic material $Na_4Ir_3O_8$, which realizes an hyper-kagome antiferromagnet, in which spin-1/2 moments reside on a three-dimensional network of corner-sharing triangles[7]—see Fig. [1]. None of these compounds exhibit indications of magnetic ordering. The interpretation of the first two materials, however, is complicated by the appearance of inhomogeneous magnetic moments at low temperature in $\kappa\text{-}(ET)_2Cu_2(CN)_3$,[8] and by fairly high levels of substitutional disorder (Zn for Cu) in $ZnCu_3(OH)_6Cl_2$. By contrast, the Ir^{4+} moments are expected to be well ordered in $Na_4Ir_3O_8$ due to the much larger ionic radius of Ir compared to Na and O.

Two recent works[9,10] assumed a nearest-neighbor antiferromagnetic Heisenberg model for $Na_4Ir_3O_8$. In Ref. [9], the authors treated the spins as classical $O(N)$ vectors. In Ref. [10], the authors employed a large-N $Sp(N)$ method. We will discuss the results of these papers in relation to our own in Sec. VII.

The principal objective of this paper is to take a step back and reconsider the appropriate *model* for $Na_4Ir_3O_8$. Due to the large atomic number ($Z = 77$) of Ir, however, we must carefully treat spin-orbit coupling, whose leading effect in localized $S = 1/2$ electron systems is the Dzyaloshinskii-Moriya (DM) interaction in the weak spin-orbit coupling limit. In fact, DM interactions have been argued to play an important role even in $ZnCu_3(OH)_6Cl_2$, with much less relativistic Cu ($Z = 29$) moments.[11] The DM interaction reduces
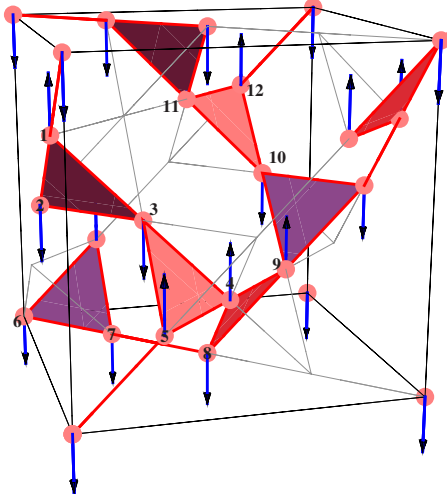
FIG. 1. (Color online) The hyper-kagome lattice of Ir^{4+} spins, with one classical ground state of the strong anisotropy Hamiltonian shown. Although this particular ground state is collinear, other ground states are not.

the full SU(2) spin-rotational invariance of the Heisenberg Hamiltonian to the Z_2 discrete time-reversal symmetry (in addition to coupling spin transformations to the discrete point-group operations of the lattice). On general grounds, this is expected to lower the degeneracy of the classical ground-state manifold. However, depending upon the detailed form of the DM coupling, varying degrees of degeneracy remain, indicative of different amounts of frustration. The tendency of the system to retain the order of the classical ground state is certainly also variable, and warrants investigation. This is one of the motivations of the present study.

Another motivation comes directly from the experiments in Ref. 7, several aspects of which are suggestive of the presence of spin-orbit coupling. First, the "Wilson ratio" $R = T\chi/c_v$ is observed to *grow* with cooling at low temperature, following a power law $R \sim 1/T^{\alpha-1}$, with $2 < \alpha < 3$. Here $\chi \sim$ const is the magnetic susceptibility and $c_v \sim T^\alpha$ is the specific heat. As will be discussed in Sec. II, such a low-temperature behavior is incompatible with *any* spin-rotationally invariant phase of matter supporting well-defined quasiparticle excitations. To our knowledge, it is at odds with all known theoretical models of quantum spin liquids, and seems highly unlikely on general grounds. Taking into account the observed field independence (up to 12 T) of the specific heat c_v brings the behavior even further into disagreement with spin-rotationally invariant theories. Second, samples in which a fraction x of Ir atoms are substituted by Ti (which are in a no-magnetic Ti^{4+} state) display a Curie component in the susceptibility linearly proportional to x with a *strongly suppressed amplitude*, of approximately 1/3 of a spin-1/2 moment per Ti. As we also show in Sec. II B, such behavior is also at odds with any *simple* spin-rotationally invariant low-temperature phase (assuming no clustering of the Ti atoms), though some more exotic. All these observations, however, are readily reconciled by assuming the presence of spin-rotational symmetry breaking. Given the lack of any observed magnetic ordering, explicit

and substantial spin-orbit interactions would appear to be a likely candidate.

In Sec. III, we consider an explicit semi-microscopic calculation of the exchange Hamiltonian in the presence of spin-orbit coupling. We consider both superexchange through the intermediate O atoms, and direct exchange between closest pairs of Ir spins. The results depend crucially upon the relative magnitude of the spin-orbit coupling constant λ and the noncubic splittings of the t_{2g} multiplet. This is quantified by two dimensionless ratios of λ to the two energy splittings $\epsilon_2 - \epsilon_1$ and $\epsilon_3 - \epsilon_1$ of the orbital levels in the absence of spin orbit. When λ is the largest energy scale—the "strong spin-orbit limit"—the "spin" has a substantial orbital angular momentum component, while in the opposite "weak spin-orbit limit," it is predominantly microscopic spin angular momentum. Indeed, the g factor has *opposite* sign in the two limits. Which if either limit applies is the most fundamental physical question to be understood concerning the nature of magnetism in $Na_4Ir_3O_8$. We are not aware of any calculations or direct experimental measurements that indicate whether $Na_4Ir_3O_8$ is in the weak or strong spin-orbit limits, or intermediate between these situations. Instead we will address this question by comparing the expected phenomenology for the two cases to experimental observations.

In the strong spin-orbit limit, when the dominant mechanism is Ir-O-Ir superexchange, we find a highly anisotropic effective spin Hamiltonian, in which two spin components on each bond interact antiferromagnetically while the third interacts ferromagnetically. Specifically,

$$\mathcal{H} = \sum_{\langle ij \rangle} J \epsilon_{ij}^\mu S_i^\mu S_j^\mu, \tag{1}$$

where $(\epsilon_{ij}^x, \epsilon_{ij}^y, \epsilon_{ij}^z)$ is a permutation of $(+1, +1, -1)$ chosen appropriately for each bond (see Sec. III F) to specify the two antiferromagnetic and one ferromagnetic direction. We call Eq. (1) the "strong anisotropy" Hamiltonian.

Somewhat surprisingly, the remaining three cases—strong spin orbit and direct exchange, weak spin-orbit and superexchange, *or* direct exchange—all lead to approximately isotropic Heisenberg interactions. For the weak spin-orbit limit, this is guaranteed, but it is certainly not in the strong spin-orbit case. The dominant spin-rotational symmetry-breaking effect, which is perturbative in all three regimes, is the DM interaction. The effective Hamiltonian has the form

$$\mathcal{H} = \sum_{\langle ij \rangle} [J\mathbf{S}_i \cdot \mathbf{S}_j + \mathbf{D}_{ij} \cdot (\mathbf{S}_i \times \mathbf{S}_j)]. \tag{2}$$

Here J is the same for all bonds, and estimated as $J \approx 400$ K from the measured Curie-Weiss temperature $\Theta_{CW} \approx -650$ K. Symmetry strongly restricts the structure of this effective magnetic Hamiltonian for hyper-kagome. The full set of DM vectors $\mathbf{D}_{ij}$ may be fixed by just three parameters. That is, $\mathbf{D}_{ij}$ on any one bond is arbitrary (by symmetry), but that choice determines all remaining $\mathbf{D}_{ij}$ in the system. It is convenient to choose the local coordinate system (D_1, D_2, D_3), where D_1 is the component aligned with the bond, D_2 is normal to the triangle plane in hyper-kagome lattice, and D_3 lies in the triangle plane but perpendicular to the bond (see Fig. 3). The semi-microscopic calculations in

Sec. III G confirm that all three components are nonvanishing, and give a quantitative understanding of them. Due to the large λ and considerable uncertainties in estimating the noncubic energy splittings, it is difficult to estimate the overall magnitude of the DM terms, but there is no reason they need be particularly small, though the perturbative estimates are presumably valid only for $|D_i| < J \lesssim 0.1$ or so. A naive estimation is obtained by noting that in this limit the ratios of DM to exchange are expected to be of the same order as the shift of the g factor, i.e., $|D_i|/J \sim |1 - |g|/2|$. From the measured moment $\mu_{\mathrm{eff}} \approx 1.9 \mu_B = |g| \mu_B$, assuming we are in this limit would give $|D_i|/J \sim 0.05$ or so.

In Sec. IV, we considered the strong anisotropy Hamiltonian, Eq. (1) in the classical approximation. Remarkably, unlike the Heisenberg model, which is macroscopically degenerate (i.e., its ground states are specified by a number of continuous parameters proportional to the number of spins), the system in this limit has an almost unique ground state. We find a continuous *two parameter* manifold of ground states, in which any one spin can be specified arbitrarily, after which all others are determined. This is still a small accidental degeneracy, since the system has itself only discrete (space-group and time-reversal) symmetries which do not protect any continuous degeneracies. Nevertheless, this degeneracy is presumably insufficient to prevent ordering in a classical system. The behavior in the physical $S = 1/2$ quantum problem is not known, but one would expect that an ordered phase of the same symmetry as the classical one is rather likely, and there is little reason to suppose a significant suppression of the ordering temperature relative to the Curie-Weiss scale. The disagreement of these expectations with the experimental observations suggests that it is the weakly anisotropic DM Hamiltonian rather than this one which is most appropriate. We however return to this question in more detail in Sec. VII.

In Sec. V, we turn to the weak anisotropy limit, and first explore the classical phase diagram of Eq. (2). In general, even this optimization problem is highly nontrivial, given the large unit cell of the hyper-kagome lattice, and the possibility that the magnetic unit cell of the ground states may be yet larger. In the special case $D_1 = D_3 = 0$ and $D_2 < 0$, however, it is possible to solve this problem exactly. The degeneracy is broken *completely* to a single Kramer's pair of coplanar ground states, for which the magnetic unit cell is equal to the crystallographic one. These may in this sense be considered $\mathbf{k} = (0,0,0)$ states. One is drawn in Fig. 2. We call this the "windmill" state. By several approximate methods, we establish the form of the phase diagram in the general D_1-D_2-D_3 parameter space. Generically the windmill state distorts to a "canted windmill" state [still with $\mathbf{k} = (0,0,0)$], occupying a finite region of the phase diagram. In addition, one finds a wide range of incommensurate phase, in which the ordering wave vector $\mathbf{k}$ is nonzero and generically irrational in reciprocal lattice coordinates. Owing to the breaking of space-group symmetries, the incommensurate phase retains more of the frustration-induced degeneracy.

A key question is whether the DM interactions, expected on physical grounds and invoked phenomenologically to explain the experimental properties discussed above, are consistent with the observed spin liquid behavior of Na$_4$Ir$_3$O$_8$,
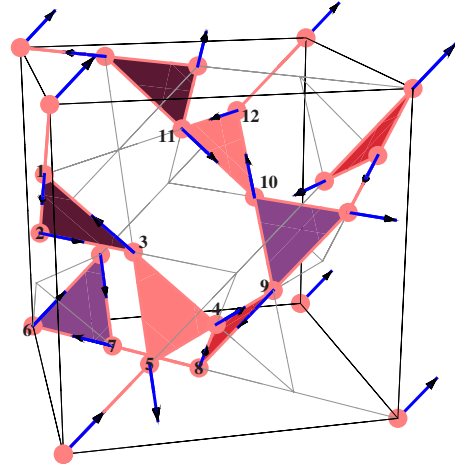

FIG. 2. (Color online) The "windmill" state, which is the classical ground state in the weak anisotropy limit when $D_2 < 0$. It is also the basis vector ψ_2 (Table V) of one-dimensional representation $\Gamma_2^{(1)}$ [see Eq. (62)]. In the generic system with nonzero D_1, D_3 the spins are slightly canted out of the plane of each triangle.

i.e., the lack of any ordering down to the very low temperatures of $T \approx 1.8$ K $= \Theta_{\mathrm{CW}}/360$. The breaking of degeneracy by DM might be expected to reduce quantum fluctuations and thereby lead to ordering, in conflict with experiment. To study this possibility, we carried out spin-wave calculations of the excitation gap and the quantum correction to the classical ordered moment. Indeed, we find that deep inside the $\mathbf{k} = (0,0,0)$ phases, the quantum correction is not too large, which leads us to expect that the spin-1/2 system exhibits the classical order. However, we find very large quantum corrections elsewhere in the phase diagram, even for fairly substantial $|D_i|$. In our results, a small excitation gap will lead to a large quantum correction to classical ordered moment. Decreasing the excitation gap by changing the DM vector will eventually destroy the classical ordered moment completely. In this regime, the large quantum effects invalidate the spin-wave treatment and indeed leave open the possibility of a quantum spin liquid, consistent with experiment. To further confirm the results and treatment of spin-wave theory, we implemented exact diagonalization on a small cluster (six triangles with 13 spins). The excitation gap obtained from numerical data of specific heat qualitatively agrees with the prediction of spin-wave theory.

The remainder of this paper is organized as follows. In Sec. III we discuss the symmetry allowed DM vector components and calculate the exchange spin Hamiltonian with a microscopic theory for both strong and weak spin-orbit coupling. In Sec. IV we discuss the classical ground states of the strong anisotropic exchange Hamiltonian obtained from Ir-O-Ir superexchange in the strong spin-orbit coupling limit. In Sec. V we will turn to look at the weak anisotropy Hamiltonian, namely, the nearest-neighbor Heisenberg model with small DM interactions. We first present the magnetic ordered state when $D_2 < 0$ then discuss the more general case when nonvanishing D_1 and D_3 components are present in the system. In Sec. VI, we present a linear spin-wave theory to find the zero temperature quantum correction to the magnetically ordered phase and compare with exact diagonalization. Fi-

nally, a discussion of our main results and their relevance to $Na_4Ir_3O_8$ is given in Sec. VII.

II. THERMODYNAMICS OF SPIN-ROTATIONALLY INVARIANT MAGNETIC PHASES

In this section, we discuss some apparent constraints on the low-temperature susceptibility and specific heat in spin-rotationally invariant phases of matter. As described in the introduction, these constraints appear to be violated in $Na_4Ir_3O_8$, which we take as an indication of the presence of substantial spin-orbit interactions.

A. Clean system

We take spin-rotational invariance to mean the existence of global SU(2) spin symmetry. According to standard quantum mechanics, this implies that all states may be chosen as eigenstates of S^2_{TOT} and S^z_{TOT}, where $\vec{S}_{TOT}$ is the operator for total spin. The choice of z axis being arbitrary, we take it along the axis of any applied field. The effect of the field on the system is then entirely described by the term

$$\mathcal{H}_H = -H\sum_i S^z_i = -HS^z_{TOT}, \tag{3}$$

where we have absorbed the (presumed known) g factor, Bohr magneton, etc. into the definition of H. One observes from Eq. (3) that $\mathcal{H}_H$ is diagonal in the S^z_{TOT} basis, and thus the Hamiltonian eigenstates themselves *are independent of field*, and only the eigenvalues change. Focusing on the states rather than their energies, we may say that the only effect of the field upon the system in equilibrium is to modify the occupation probabilities of states. In this sense, the magnetic field is a thermodynamic perturbation, and the susceptibility is a thermodynamic quantity, determined only by the density of states. The specific heat is of course also such a thermodynamic quantity, determined from the same density of states. Thus they are connected.

Specifically, the specific heat is a measure of the full density of states for all excitations above the ground state, irrespective of their spin quantum numbers. The susceptibility, however, only counts those excitations which carry nonzero spin S^z along the field. The possibility of spinless excitations allows some independence of the two: by introducing more $S^z=0$ states, one can increase c_v arbitrarily while leaving χ unchanged. However, the converse is not true. It would seem difficult to increase χ without also contributing to c_v. The only way in which this can be done is to introduce states with very large S^z (which then contribute a large amount to χ) but very low energy (and hence do not contribute much to c_v). This case corresponds to a system on the verge of a ferromagnetic instability.

Without fine tuning to such a point, we are led to expect that, in the presence of SU(2) symmetry, the Wilson ratio,

$$R = \frac{T\chi}{c_v}, \tag{4}$$

should have an *upper* bound, corresponding to all excitations contributing both to χ and c_v. This can indeed be shown

provided we assume the system can be described by a non-magnetic ground state and noninteracting quasiparticles characterized by a spin S^z quantum number. We define the density of state $g^b_m(\epsilon)$ and $g^f_m(\epsilon)$ for boson or fermion excitations carrying spin $S^z=m$, respectively. The specific heat is

$$c_v = \partial_T \sum_m \int_0^\infty d\epsilon \, \epsilon [g^b_m(\epsilon)n_b(\epsilon) + g^f_m(\epsilon)n_f(\epsilon)], \tag{5}$$

where

$$n_{b/f}(\epsilon) = \frac{1}{e^{\beta\epsilon} \mp 1}. \tag{6}$$

One obtains

$$c_v = \frac{k_B^2 T}{4}\sum_m \int_0^\infty dx \, x^2 \left[\frac{g^b_m(k_B Tx)}{\sinh^2(x/2)} + \frac{g^f_m(k_B Tx)}{\cosh^2(x/2)}\right]. \tag{7}$$

Now consider the susceptibility

$$\chi = \partial_H \sum_m \int_0^\infty d\epsilon \, m[g^b_m(\epsilon)n_b(\epsilon - Hm) + g^f_m(\epsilon)n_f(\epsilon - Hm)]|_{H=0}. \tag{8}$$

One finds

$$\chi = \frac{1}{4}\sum_m m^2 \int_0^\infty dx \left[\frac{g^b_m(k_B Tx)}{\sinh^2(x/2)} + \frac{g^f_m(k_B Tx)}{\cosh^2(x/2)}\right]. \tag{9}$$

In the low-temperature limit, we may approximate $g^{f/b}_m(k_B Tx)$ by its small argument behavior, which is usually a power-law form:

$$g^{b/f}_m(\epsilon) \sim A^{b/f}_m \epsilon^{\gamma^{b/f}_m}. \tag{10}$$

One needs obviously $\gamma^{f/b}_m > -1$ for the density of states to be integrable (and hence the cumulative distribution well defined). We will encounter problems with Eq. (9) if $\gamma^b_m \leq 1$ for any $m \neq 0$. This could be fixed by the inclusion of a chemical potential, whose temperature dependence we have ignored, and as usual is necessary to avoid Bose condensation of free bosons at low T when their energy is close to zero. This effect, however, does not change any of the results, so we have excluded it for simplicity here.

Given Eq. (10), the specific heat will be controlled at low T by the minimum exponent over *all* $\gamma^{b/f}_m$:

$$\gamma_0 = \min\{\gamma^{b/f}_m\}. \tag{11}$$

One has

$$c_v \sim A_0 k_B^{2+\gamma_0} T^{1+\gamma_0}, \tag{12}$$

with some constant A_0. The susceptibility is controlled by the minimum exponent for $m \neq 0$:

$$\gamma_1 = \min\{\gamma^{b/f}_m; \quad m \neq 0\}. \tag{13}$$

Note that by definition, $\gamma_0 \leq \gamma_1$. Then

$$\chi \sim A_1 T^{\gamma_1}. \tag{14}$$

Then the Wilson ratio becomes

$$R \sim R_0 T^{\Upsilon}, \tag{15}$$

where $R_0 = \frac{A_1}{A_0 k_B^{2+\gamma_0}}$ and

$$\Upsilon = \gamma_1 - \gamma_0 \geq 0. \tag{16}$$

Because $\Upsilon \geq 0$, the Wilson ratio cannot diverge on lowering T, and unless $\Upsilon = 0$, actually vanishes as $T \to 0$. In defining the Wilson ratio, we have considered only the zero-field specific heat. In a field, contributions from all excitations with $m \neq 0$ will be field dependent. So unless the $m = 0$ mode is dominant in c_v, the specific heat should be expected to be field dependent. Conversely, field independence of the specific heat requires that the $m = 0$ excitations dominate c_v. In this case, we have $\Upsilon > 0$, and the equality is *not* satisfied. Thus a field-independent low-temperature specific heat would be expected to correspond to a *vanishing* Wilson ratio as $T \to 0$. This makes the observed *divergence* of R on lowering T in Na$_4$Ir$_3$O$_8$ even more at odds with the theoretical expectation for an SU(2) invariant system.

A few comments are in order. First, while we have assumed power-law forms for the low-energy density of states, this is not essential. We believe the lack of low-temperature divergence in $R(T)$ is very robust within the quasiparticle picture. Beyond the quasiparticle approximation, the situation is less clear, and we do not have a definitive proof of this behavior of $R(T)$. However, we do not know of any theoretical counter-examples in the literature for SU(2) invariant low-temperature phases.

If SU(2) symmetry (or more specifically, invariance under spin rotations about the measurement axis) is broken, however, one readily and indeed almost generically observes this behavior. This is quite familiar from the case of ordered antiferromagnets in two or three dimensions. These are well known to display a nonvanishing constant zero-temperature uniform susceptibility χ_0 and a power-law specific heat $c_v \sim AT^d$ due to spin-wave excitations, hence a Wilson ratio obeying Eq. (15) with however $\Upsilon = 1 - d < 0$. This arises because the ground state itself is modified continuously by the introduction of a magnetic field. Semiclassically, the magnetic field leads to a smooth canting of the antiferromagnetic moments in the field direction, linearly proportional to the applied field.

This phenomenon is, however, not limited to systems with spontaneous symmetry breaking. It occurs whenever the effective Hamiltonian for the low-temperature phase does not conserve the spin component along the magnetic field. As an extreme example, one may consider the case of two spin-1/2 spins coupled together by antiferromagnetic exchange and DM interaction:

$$\mathcal{H}_2 = J\mathbf{S}_1 \cdot \mathbf{S}_2 - D\hat{\mathbf{z}} \cdot \mathbf{S}_1 \times \mathbf{S}_2 - H(S_1^x + S_2^x), \tag{17}$$

where we have chosen the DM vector along the z axis, and therefore oriented the field along x so that it couples to a nonconserved magnetization. One can readily diagonalize the Hamiltonian and find that in zero field it has a unique ground state with a gap $\Delta = 1/2(J + \sqrt{J^2 + D^2})$. Nevertheless, the susceptibility is nonzero when $D \neq 0$:

$$\chi = \left. \frac{\partial S_i^x}{\partial H} \right|_{H=0} = \frac{\sqrt{J^2 + D^2} - J}{J(\sqrt{J^2 + D^2} + J)}. \tag{18}$$

Because of the gap, the specific heat of the dimer is activated at low temperature, and hence the dimer's Wilson ratio diverges *exponentially* at low temperature. In general, a nonzero limit for the low-temperature susceptibility is always to be expected once SU(2) symmetry-breaking perturbations are taken into account. The specific heat, however, is insensitive to symmetry, and remains a true probe of low-energy modes.

B. Impurity susceptibility

In Na$_4$Ir$_3$O$_8$, the introduction of nonmagnetic impurities (substitution of Ti^{4+} for Ir^{4+}) was observed to give rise to a Curie component with a reduced effective moment of $\mu_{\text{eff}} \approx (2\mu_B)/3$ per Ti. We would like to argue that a spin liquid state with such a large reduction from the moment of a free spin, $2\mu_B$, is unlikely in the absence of spin-orbit interactions, but quite likely when they are invoked.

Suppose the Hamiltonian has global SU(2) spin rotational symmetry in the absence of an applied magnetic field. Then a spin liquid ground state, which, by definition, does not break SU(2) symmetry, must be a spin singlet, i.e., a state of total spin $S = 0$. Its excitations can therefore by characterized by spin quantum numbers. Representations of SU(2) always have integer or half-integer spin, and in particular for all these the projection of the total spin along any field axis is a multiple of 1/2.

Now consider a single impurity. It may be a strong perturbation locally, but does not perturb the Hamiltonian far from itself. Again presuming spin orbit can be neglected, the ground state of this system should be a spin eigenstate, although not necessarily nonzero. Nevertheless, it can be classified by a total spin which is a multiple of half an integer. It is natural to expect that the ground-state multiplet of a single impurity controls the impurity susceptibility (but see below). Allowing now for an external field, this is simply described as in the previous subsection by Eq. (3). Since the low-energy states are still good representations of SU(2), and only the total spin projection enters Eq. (3), we will obtain an effective moment which is at a minimum (if it is nonzero) $2\mu_B$ per impurity.

The caveat in this argument is the possibility of a Kondo-like effect. If the spin liquid state is gapless, then there is a possibility for an impurity moment to be "screened" by the bulk degrees of freedom. Still, the possibility of a fractional impurity moment is delicate. Most Kondo effects either completely screen the moment (as in the single-channel case, leading to $\mu_{\text{eff}} = 0$) or to weaker temperature dependence of the impurity susceptibility (e.g., $\chi_{\text{imp}} \sim |\ln T|$ in the two-channel model, which has a nontrivial Kondo fixed point). Thus most types of Kondo effect do not allow for such behavior. Recently, it has been suggested that some spin liquids might sustain a *critical fixed line* of Kondo fixed points, connected to the free impurity fixed point. This situation can in fact lead to a renormalized Curie constant.[12] It would indeed be appealing should such an exotic possibility be realized in

$Na_4Ir_3O_8$, but we should allow for simpler explanations.

As is well known, the effective moment of ions in solids varies widely from the quantized values expected from SU(2) symmetric considerations. This is of course due to spin-orbit coupling. In general, with spin-orbit interactions present, the ground state of an impurity can be expected to be a Kramer's singlet or a Kramer's doublet. In the latter case, it will behave energetically (i.e., in specific heat) as a spin-1/2 spin, but will have in general a nontrivial g tensor describing its coupling to a field. This reflects a change in the effective moment. Thus there is no "quantization" of the effective moment once spin-orbit coupling is substantial. The observed fractional effective moment in $Na_4Ir_3O_8$ is perhaps another indication in this direction.

III. SPIN-ORBIT COUPLING IN THE HYPER-KAGOME LATTICE

In this section, we discuss the form of the spin-orbit modifications to the isotropic Heisenberg Hamiltonian. This is not directly calculable from semi-microscopic considerations without some assumptions about the local energetics due to crystal field splittings. Therefore we consider below a number of cases.

A. Symmetry-allowed DM vector components

In several cases, we will find that the dominant effect of spin-orbit coupling is to induce DM interactions between the nearest-neighbor spins. Therefore before attempting any calculations, it is instructive to first consider the symmetry constraints upon them. Generally, DM interactions are rather highly constrained. For instance, they are absent if there is an inversion center between the two spins in question (this is not the case in $Na_4Ir_3O_8$). The compound $Na_4Ir_3O_8$ has cubic symmetry, described by the space group $P4_132$, and consequently has a number of point-group symmetries. For our purposes, it is useful to consider an unconventional set of generators of these symmetries. Specifically, the full point group can be generated from the set of 180° rotations around a local C_2 axis at each site. Due to this symmetry, all the hyper-kagome sites and bonds are equivalent. In Table V, we list the directions of the C_2 axes (ψ_1) for every site in the unit cell (see Fig. 3 for the labeling). The C_2 rotational symmetries relate the DM vectors of any two bonds. That is, given the DM vector on any one hyper-kagome bond, all others are determined. This one DM vector, however, is itself entirely unconstrained by the P_132 symmetry.

Since any single bond of the hyper-kagome is uniquely associated with one triangle, it is natural to adopt a local coordinate system based on this triangle to describe the DM vector's components. We denote the component aligned with the bond D_1, the component normal to the triangle plane D_2, and the component normal to the bond but localized in the triangle plane D_3. Three components have been illustrated in Fig. 3. If we select the direction of D_1 component axis by assigning a direction to one bond (arrows in Fig. 3), the C_2 rotation symmetry can generate the equivalent D_1 axis for other bonds (see Fig. 3). In every triangle, there is a chirality
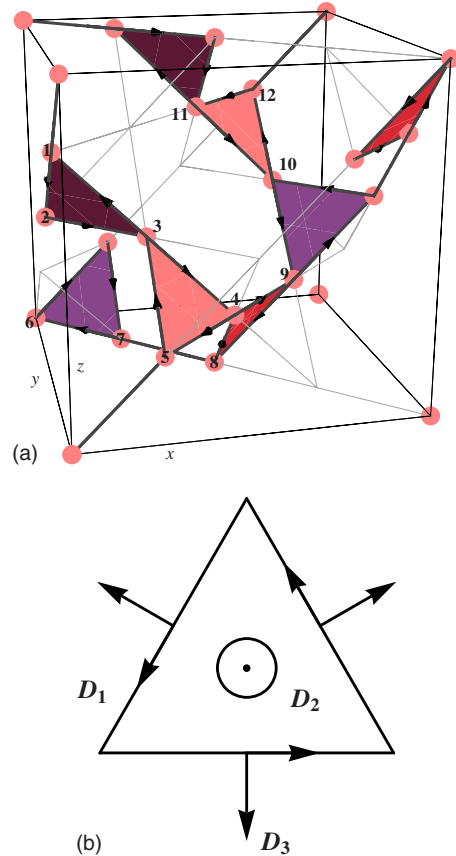

FIG. 3. (Color online) Left: One unit cell of the hyper-kagome lattice. The pink balls are occupied by magnetic ions, which are connected by dark black bonds. There are 12 sites in one primitive unit cell. The arrow from site i to site j corresponds to $\mathbf{D}_{ij} \cdot (\mathbf{S}_i \times \mathbf{S}_j)$ in the Hamiltonian. We will call these arrows DM interaction path. Right: DM vector components illustrated on one triangle. D_1 is the component which is aligned with the DM interaction path (left). D_2 is the component normal to the triangle plane. The direction is decided by the chirality of bond direction. D_3 is the component perpendicular to the bond but in the triangle plane.

of the D_1 axis of three edges, which can be considered as the direction of D_2 axis. The cross product of D_1 and D_2 directional vector generates the direction of D_3 axis.

Such a parametrization may be applied not only for the hyper-kagome lattice, but for any lattice consisting of corner-sharing triangles, such as the slightly distorted kagome lattice of Fe/Cr-jarosites.[13–15] In that example, the D_1 component is forbidden by a mirror plane symmetry. In $Na_4Ir_3O_8$, there are as we said no constraints on the D_i, and we might naively expect all three components to be nonvanishing and comparable. We will investigate this by microscopic calculations below.

B. Local electron energetics of Ir ion

Before moving to the microscopic theory of spin-orbit interactions, we need to understand the electron energy levels of the Ir^{4+} ions. With coordinates taken from Table I in Ref. 7, two Ir^{4+} and their surrounding O^{2-} are drawn in Fig. 4. For A ion, the C_2 axis orients along $\frac{1}{\sqrt{2}}(1, -1, 0)$. Under

TABLE I. The parity sectors of $5d$ electron orbitals by C_2 rotation.

State	$5d$ orbitals at A	$3d$ orbitals at B	Parity
$|1\rangle$	xy	yz	even
$|2\rangle$	$\frac{1}{\sqrt{2}}(xz-yz)$	$\frac{1}{\sqrt{2}}(yx+zx)$	odd
$|3\rangle$	$\frac{1}{\sqrt{2}}(xz+yz)$	$\frac{1}{\sqrt{2}}(yx-zx)$	even
$|4\rangle$	x^2-y^2	y^2-z^2	odd
$|5\rangle$	$3z^2-r^2$	$3x^2-r^2$	even

this symmetry operation, $x\rightarrow-y$, $y\rightarrow-x$, and $z\rightarrow-z$. Accordingly, we can group the $5d$ orbitals into even and odd parity sectors, as shown in Table I.

A large cubic crystal field splits the e_g and t_{2g} states. The surrounding O^{2-} octahedron is slightly distorted to further split all the three t_{2g} states. Ultimately no degeneracy is protected because the C_2 symmetry has only one-dimensional irreducible representations. The energetic ordering of orbitals shown in Fig. 5 was determined by looking at Coulomb interaction from surrounding O^{2-} and ignoring the spin-orbit interaction.

C. Microscopic theory of exchange spin Hamiltonian

Although symmetry determines the allowed nonzero components of the Dzyaloshinskii-Moriya (DM) interaction, it does not give any guidance as to their relative and absolute magnitudes.[13,16,17] In this part, we will derive the exchange spin Hamiltonian from a microscopic point of view and obtain expressions from which crude estimates of the magnitude of various terms can be obtained.[13,16,17] We consider both the hopping between Ir and O orbitals, and direct hop-
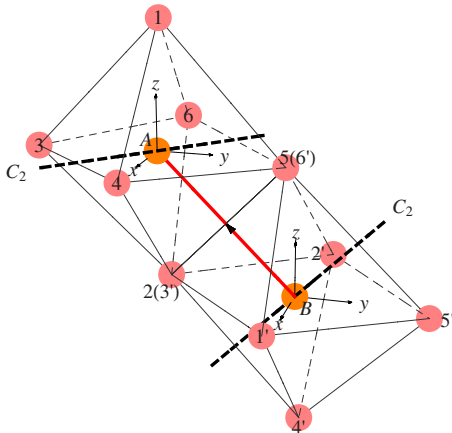

FIG. 4. (Color online) Ir^{4+} and octahedron O^{2-} environment (thin black line). Two neighboring Ir^{4+} are denoted by A and B (in orange). A/B's six O^{2-} are labeled as $1/1'$, $2/2'$, $3/3'$, $4/4'$, $5/5'$, and $6/6'$ (in pink), in which, 2 and $3'$, 5 and $6'$ label the same points. The distances between Ir^{4+} and O^{2-} order this way: $|A5| = |B5'| = |B6'| > |A3| = |A4| = |B3'| = |B4'| > |A1| = |A2| = |B1'| = |B2'|$. The C_2 axis (thick dash line) orients along $\frac{1}{\sqrt{2}}(1,-1,0)$ at Ir^{4+} A and $\frac{1}{\sqrt{2}}(0,1,1)$ at Ir^{4+} B. Mapped to the ideal hyper-kagome lattice, A and B correspond to point 4 and 8 in Fig. 3, respectively.
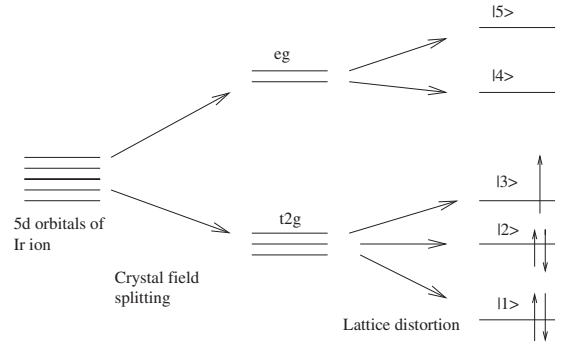

FIG. 5. The splitting and electron occupation of $5d$ orbitals of Ir^{4+} ions in the absence of spin-orbit interaction. The states are defined in Table I.

ping between Ir orbitals. We also assume that the e_g-t_{2g} splitting is much greater than the splittings among the three t_{2g} states so that we can completely project out the two e_g states. The model is then of five electrons on the t_{2g} orbitals of every Ir^{4+}. Following some notations in Ref. 17, we can write the Hamiltonian of the Ir and O sublattice as

$$\mathcal{H} = \mathcal{H}_0 + \mathcal{H}_t + \mathcal{H}_{LS}, \quad (19)$$

where,

$$\mathcal{H}_0 = \sum_{jm\sigma} \epsilon_m d^\dagger_{jm\sigma} d_{jm\sigma} + \sum_{kn\sigma} \epsilon_{p_n} p^\dagger_{kn\sigma} p_{kn\sigma}$$

$$+ \frac{U_d}{2} \sum_{jmm'\sigma\sigma'} d^\dagger_{jm\sigma} d^\dagger_{jm'\sigma'} d_{jm'\sigma'} d_{jm\sigma}$$

$$+ \frac{U_p}{2} \sum_{knn'\sigma\sigma'} p^\dagger_{kn\sigma} p^\dagger_{kn'\sigma'} p_{kn'\sigma'} p_{kn\sigma}, \quad (20)$$

$$\mathcal{H}_t = \sum_{jm\sigma} \sum_{k(j)n} (t_{jm,kn} d^\dagger_{jm\sigma} p_{kn\sigma} + \text{H.c.})$$

$$+ \sum_{\langle jj'\rangle} \sum_{mm'} t^d_{jm,j'm'} d^\dagger_{jm\sigma} d_{j'm'\sigma}, \quad (21)$$

$$\mathcal{H}_{LS} = \lambda \sum_j \boldsymbol{\ell}_j \cdot \boldsymbol{s}_j. \quad (22)$$

$k(j)$ denotes the O^{2-} of the neighboring Ir^{4+} site j, $d^\dagger_{jm\sigma}$ is the creation operator of an electron with spin σ of the mth $5d$ orbital of ith Ir ion, and ϵ_m is the energy of this orbital. m will take 1, 2, and 3. $p^\dagger_{kn\sigma}$ is the creation operator of an electron on the $2p_n$ orbital with spin σ. The energies are measured from the lowest energy level of the Ir $5d$ orbitals, and U_d and U_p are the Coulomb interaction constants between holes on the Ir^{4+} site and O^{2-} site, respectively. We assume that U_d and U_p are orbital independent and ignore other "Kanamori parameters:"[18] the interorbital exchange coupling and the pair-hopping amplitude, which should be small compared to Coulomb interaction. We also ignore the Coulomb interaction between two electrons on different intermediate O^{2-} ions. Here $t_{jm,kn}$ denotes the transfer of an electron between the mth orbital of Ir^{4+} ion j and one of the $2p_n$ orbitals of the neighboring O^{2-} ions k. Similarly, $t^d_{jm,j'm'}$

is the matrix element for electron transfer between m and m' orbitals on two nearest-neighbor (in the hyper-kagome sense) Ir atoms. ℓ_j and $\mathbf{s}_j$ denote the orbital and spin angular momenta at the jth Ir^{4+} ion, respectively, and λ is the spin-orbit coupling constant of the Ir^{4+} ion.

In order to understand the electron occupation on each site, we collect the quadratic terms for each site in Eq. (22) and write down the onsite Hamiltonian as

$$\mathcal{H}^{(i)} = \sum_{mm'\sigma\sigma'} d^{\dagger}_{im\sigma} \mathcal{M}^{(i)}_{m\sigma,m'\sigma'} d_{im'\sigma'} \qquad (23)$$

with

$$\mathcal{M}^{(i)}_{m\sigma,m'\sigma'} = \epsilon_m \delta_{\sigma\sigma'} \delta_{mm'} + \lambda \boldsymbol{\ell}_{imm'} \cdot \mathbf{s}_{\sigma\sigma'}, \qquad (24)$$

where $\boldsymbol{\sigma}$ is the Pauli matrix and $\mathbf{L}_{imm'}$ is the matrix element of $\mathbf{L}_i$ between the mth and m'th orbital of the ith Ir^{4+} ion. It is useful to note[19] that the vector of three-dimensional matrix orbital angular momentum operators projected into the t_{2g} manifold is actually proportional to the vector of orbital angular momentum operators for the three ordinary (p_x, p_y, p_z) states, but with a proportionality constant of -1. That is, suppressing the m, m' indices,

$$\boldsymbol{\ell}_i = -\mathbf{L}_i, \qquad (25)$$

where $\mathbf{L}$ is a canonical angular momentum operator with $\mathbf{L}^2 = \ell(\ell+1) = 2$. This effectively makes the spin-orbit coupling term directly analogous to the familiar one from an isolated atom with spherical symmetry in a p shell, but with the sign of the spin-orbit coupling reversed.

D. Strong and weak spin-orbit limits

Obviously the nature of the "spin" itself (i.e., the Kramer's doublet ground state of the single hole in this multiplet) is crucially dependent upon the strength of the spin-orbit interaction, relative to the noncubic splittings $\epsilon_3 - \epsilon_2$, $\epsilon_3 - \epsilon_1$. This determines the nature of the *wave functions* of the Kramer's pair, for instance the degree to which the "spin" carries true electron spin angular moment or instead orbital angular momentum. This is more fundamental than the exchange interaction so we consider it first.

1. Strong spin orbit

In the strong spin-orbit limit, we can to a first approximation ignore the noncubic splittings, and we have simply

$$\mathcal{M}^{(i)} = \lambda \boldsymbol{\ell}_i \cdot \mathbf{s}_i = -\lambda \mathbf{L}_i \cdot \mathbf{s}_i. \qquad (26)$$

This is of course diagonalized by constructing eigenstates of the "total angular momentum"

$$\mathbf{J}_i = \mathbf{L}_i + \mathbf{s}_i. \qquad (27)$$

Because of the minus sign in Eq. (26), the highest energy doublet is simply the $j = 1/2$ Kramer's pair. This describes the wave function of the half-filled orbital. It is natural to define the effective spin operator in this case as

$$\mathbf{S}_i = \mathbf{J}_i. \qquad (28)$$

Clearly it is a strong mix of orbital and spin components. According to the Wigner-Eckart theorem, the matrix ele-

ments of $\mathbf{s}_i$, $\mathbf{L}_i$, and $\mathbf{J}_i$ are all proportional. This enables one, with a little Clebsch-Gordan algebra, to arrive at an expression for the magnetic moment operator (in the $j = 1/2$ manifold),

$$\mathbf{M}_i = -\mu_B(\boldsymbol{\ell}_i + 2\mathbf{s}_i) = +2\mu_B \mathbf{S}_i, \qquad (29)$$

where μ_B is the Bohr magneton. Interestingly, this is the same magnitude but opposite sign as for a free electron. It will of course suffer corrections perturbative in $(\epsilon_i - \epsilon_3)/\lambda$, as one moves away from the strong spin-orbit limit.

2. Weak spin orbit

Now consider the weak spin-orbit limit. In this case, for $\lambda = 0$, the half-filled doublet is simply the $m = 3$ orbital, with two possible "true" spin orientations. Thus we approximately have

$$\mathbf{S}_i \approx \mathbf{s}_i + \mathcal{O}[\lambda/(\epsilon_i - \epsilon_j)]. \qquad (30)$$

Now there is essentially no orbital angular momentum component to the spin ($\ell_i \approx 0$), and one obtains

$$\mathbf{M}_i = -2\mu_B \mathbf{S}_i \left[1 + \mathcal{O}\left(\left| \frac{\lambda}{|\epsilon_{1,2} - \epsilon_3|} \right| \right) \right]. \qquad (31)$$

Note the important sign difference from Eq. (29). This is the most fundamental physical distinction between the weak and strong spin-orbit limits. However, the magnitude of the proportionality between the magnetization and spin—the g factor—is the same in both cases. This means that the simplest experimental measure, the Curie susceptibility, cannot distinguish the two possibilities. We will consider both cases below.

E. General exchange formulation

We now turn to the exchange calculations. Let us consider the general case first. We must deal with $\mathcal{M}^{(i)}$, which is a 6×6 matrix. Diagonalize $\mathcal{M}^{(i)}$ so that $\mathcal{M}^{(i)} = T^{(i)\dagger} \mathcal{E} T^{(i)}$. Here, $\mathcal{E}$ is a site-independent eigenvalue matrix, and $T^{(i)}$ is a unitary eigenvector matrix. $\mathcal{M}^{(i)}$ has three different eigenvalues $\mathcal{E}_1$, $\mathcal{E}_2$, and $\mathcal{E}_3$, each has a twofold degeneracy due to Kramers' degeneracy theorem. The effective spin operator $\mathbf{S}_i$ will be defined to act in this doublet. In the strong and weak spin-orbit limits, we have explicitly Eq. (28) and Eq. (30), respectively. Furthermore, we define a new set of electron creation and annihilation operators

$$a_{im\sigma} = T^{(i)}_{m\sigma,m'\sigma'} d_{im'\sigma'} \qquad (32)$$

with $a_{im\sigma}$ annihilates an electron on the $\mathcal{E}_m$ state with spin σ at site i.

Without losing any generality, we assume that $\mathcal{E}_3 > \mathcal{E}_{1,2}$, then $\mathcal{E}_{1,2}$ states are fully occupied and $\mathcal{E}_3$ state is half occupied, leading to a total spin-$\frac{1}{2}$ at every site. Accordingly, the magnetic momentum operator $[\mathbf{M}_i = -\mu_B(\boldsymbol{\ell}_i + 2\mathbf{s}_i)]$ at each site should be projected onto the Kramers' doublet ground states:

$$\frac{\mathbf{M}_i}{\mu_B} = -P_i \sum_{mn\alpha\beta} d^\dagger_{im\alpha}(\ell_{imn}\delta_{\alpha\beta} + \delta_{mn}\boldsymbol{\sigma}_{\alpha\beta})d_{in\beta}P_i$$

$$= -\mathbf{G}^{(i)}_{3\alpha,3\beta}\boldsymbol{\sigma}_{\beta\alpha}\cdot\mathbf{S}_i, \tag{33}$$

with $\boldsymbol{\sigma}$ the vector of Pauli matrices. Also, $\mathbf{G}^{(i)}_{l\sigma,j\delta}$ and the effective spin operator $\mathbf{S}_i$ are defined as

$$\mathbf{G}^{(i)}_{l\sigma,j\delta} = \sum_{mn\alpha\beta} T^{(i)}_{l\sigma,m\alpha}(\ell_{imn}\delta_{\alpha\beta} + \delta_{mn}\boldsymbol{\sigma}_{\alpha\beta})T^{(i)*}_{j\delta,n\beta},$$

$$\mathbf{S}_i = \sum_{\alpha,\beta}\frac{1}{2}a^\dagger_{i3\alpha}\boldsymbol{\sigma}_{\alpha\beta}a_{i3\beta}, \tag{34}$$

and P_i is the ground-state projection operator

$$P_i = a_{i3\uparrow}|\phi\rangle\langle\phi|a^\dagger_{i3\uparrow} + a_{i3\downarrow}|\phi\rangle\langle\phi|a^\dagger_{i3\downarrow}. \tag{35}$$

Here $|\phi\rangle$ is the $\mathcal{E}_{1,2,3}$ fully occupied state. In the last step Eq. (33), $\sum_\sigma a^\dagger_{i3\sigma}a_{i3\sigma}=1$ has been used.

Let's go back to Eq. (22), and express the microscopic Hamiltonian in terms of $a_{jm\sigma}$ and $a^\dagger_{jm\sigma}$. Given the Hamiltonian in Eq. (19), which includes the largest Coulomb energy U but neglects the smaller Hunds-rule exchange coupling *between* electrons in different orbitals on the same atom (and other similar interactions), only hopping through the half-filled orbital contributes to the superexchange interaction. This is in accord with the "Goodenough-Kanamori" rules, which state that the exchange coupling contributed from a half-occupied orbital and a fully occupied orbital is much weaker than the one from two half-occupied orbitals. Thus, we only need to focus on the hopping between the $\mathcal{E}_3$ orbitals as half-occupied orbital. The microscopic Hamiltonian is written as

$$\mathcal{H} = \sum_{kn\sigma}\epsilon_{p_n}p^\dagger_{kn\sigma}p_{kn\sigma} + \frac{U_p}{2}\sum_{knn'\sigma\sigma'}p^\dagger_{kn\sigma}p^\dagger_{kn'\sigma'}p_{kn'\sigma'}p_{kn\sigma}$$

$$+ \sum_{jm\sigma}\mathcal{E}_m a^\dagger_{jm\sigma}a_{jm\sigma} + \frac{U_d}{2}\sum_{jmm'\sigma\sigma'}a^\dagger_{jm\sigma}a^\dagger_{jm'\sigma'}a_{jm'\sigma'}a_{jm\sigma}$$

$$+ \sum_{jk(j)n}\sum_{\alpha\beta}[(\tilde{t}_{j3,kn}\delta_{\alpha\beta} + \mathbf{C}_{j,kn}\cdot\boldsymbol{\sigma}_{\alpha\beta})a^\dagger_{j3\alpha}p_{kn\beta} + \text{H.c.}]$$

$$+ \sum_{\langle jj'\rangle}\sum_{\alpha\beta}[(\tilde{t}^d_{j3,j'3}\delta_{\alpha\beta} + \mathbf{C}^d_{jj'}\cdot\boldsymbol{\sigma}_{\alpha\beta})a^\dagger_{j3\alpha}a_{j'3\beta} + \text{H.c.}],$$

$$\tag{36}$$

with

$$\tilde{t}_{j3,kn} = \sum_{m\sigma}\frac{1}{2}t_{jm,kn}T^{(j)}_{3\sigma,m\sigma},$$

$$\mathbf{C}_{j,kn} = \sum_{m,\alpha\beta}\frac{1}{2}t_{jm,kn}T^{(j)}_{3\alpha,m\beta}\boldsymbol{\sigma}_{\beta\alpha}, \tag{37}$$

and

$$\tilde{t}^d_{j3,j'3} = \sum_{mm',\alpha\sigma}\frac{1}{2}t^d_{jm,j'm'}T^{(j)}_{3\alpha,m\sigma}T^{(j')\dagger}_{m'\sigma,3\alpha},$$

$$\mathbf{C}^d_{jj'} = \sum_{mm',\sigma,\alpha\beta}\frac{1}{2}t^d_{jm,j'm'}T^{(j)}_{3\alpha,m\sigma}T^{(j')\dagger}_{m'\sigma,3\beta}\boldsymbol{\sigma}_{\beta\alpha}, \tag{38}$$

where $\boldsymbol{\sigma}$ is vector of the three Pauli matrices. Now we may follow the standard perturbative treatment of superexchange. We consider separately the superexchange through the intermediate O^{2-} ions, and the direct exchange contributions.

1. Superexchange through oxygen ions

In this case the leading contribution is fourth order in hopping, i.e., a result of fourth-order degenerate perturbation theory. We must include four "hops" between Ir^{4+} and O^{2-} ions, which consist of "hops" described by spin-isotropic $\tilde{t}$ matrix elements, and "hops" given by anisotropic $\mathbf{C}$ matrix elements. One thereby obtains the exchange Hamiltonian as

$$\mathcal{H}_{\text{ex}} = \sum_{\langle ij\rangle}[J\mathbf{S}_i\cdot\mathbf{S}_j + \mathbf{D}_{ij}\cdot(\mathbf{S}_i\times\mathbf{S}_j) + \mathbf{S}_i\cdot\overset{\leftrightarrow}{\Gamma}_{ij}\cdot\mathbf{S}_j], \tag{39}$$

with the first two terms the Heisenberg and DM interactions precisely as in Eq. (2), and the third term the anisotropic exchange. The explicit formulas for the coupling constants are

$$J = 4\sum_{kn,k'n'}s_{ij,kn}g_{kn,k'n'}s_{ji,k'n'}, \tag{40}$$

$$\mathbf{D}_{ij} = -4i\sum_{kn,k'n'}(\mathbf{v}_{ij,kn}g_{kn,k'n'}s_{ji,k'n'} - s_{ij,kn}g_{kn,k'n'}\mathbf{v}_{ji,k'n'}),$$

$$\tag{41}$$

$$\overset{\leftrightarrow}{\Gamma}_{ij} = 4\sum_{kn,k'n'}[(\overset{\leftarrow}{\mathbf{v}}_{ij,kn}g_{kn,k'n'}\overset{\rightarrow}{\mathbf{v}}_{ji,k'n'} + \overset{\leftarrow}{\mathbf{v}}_{ji,kn}g_{kn,k'n'}\overset{\rightarrow}{\mathbf{v}}_{ij,k'n'})$$

$$- \overset{\leftrightarrow}{1}(\mathbf{v}_{ij,kn}\cdot g_{kn,k'n'}\mathbf{v}_{ji,k'n'})]. \tag{42}$$

The vector with arrow $\leftarrow$ or $\rightarrow$ indicates that inner product is taken with the spin operator put in the direction of the arrow. $\overset{\leftrightarrow}{1}$ is a 3×3 unit matrix. $s_{ij,kn}$, $\mathbf{v}_{ij,kn}$, and $g_{kn,k'n'}$ are given by

$$s_{ij,kn} = \tilde{t}_{i3,kn}\tilde{t}_{kn,j3} + \mathbf{C}_{i,kn}\cdot\mathbf{C}_{kn,j}, \tag{43}$$

$$\mathbf{v}_{ij,kn} = \mathbf{C}_{i,kn}\tilde{t}_{kn,j3} + \tilde{t}_{i3,kn}\mathbf{C}_{kn,j} + i(\mathbf{C}_{i,kn}\times\mathbf{C}_{kn,j}), \tag{44}$$

$$g_{kn,k'n'} = \frac{\left(1 - \frac{1}{2}\delta_{kk'}\delta_{nn'}\right)(\tilde{\epsilon}_{p_{kn}}^{-1} + \tilde{\epsilon}_{p_{k'n'}}^{-1})^2}{\tilde{\epsilon}_{p_{kn}} + \tilde{\epsilon}_{p_{k'n'}} + U_p\delta_{kk'}} + (\tilde{\epsilon}_{p_{kn}}\tilde{\epsilon}_{p_{k'n'}}U_d)^{-1},$$

$$\tag{45}$$

with $\tilde{\epsilon}_{p_{kn}}=\mathcal{E}_3 - \epsilon_{p_{kn}} + 5(U_d - U_p)$. In the following subsections, we will try to estimate these exchange couplings in both the strong and weak spin-orbit interaction cases.

2. Direct exchange

Here we require only second-order perturbation theory in the direct matrix elements. One obtains the results:[16]

TABLE II. The transfer integrals between the t_{2g} orbitals on A and B Ir^{4+} and the $p_{x,y,z}$ orbitals on the intermediate O^{2-} ions. "$2p_x$" represents the p_x orbital on the second O^{2-} ion in Fig. 4, "A, xz" represents the xz orbital on the A ion, and the entry t on the row of "A, xz" and the column of "$2p_x$" denotes the hopping amplitude (transfer integral) from xz orbital at A ion to p_x orbital on second O^{2-} ion. Other notation can be understood likewise.

	$2p_x$	$2p_y$	$2p_z$	$5p_x$	$5p_y$	$5p_z$
A, xz	t	0	0	0	0	0
A, yz	0	t	0	0	0	$-t$
A, xy	0	0	0	$-t$	0	0
B, xz	0	0	0	$-t$	0	0
B, yz	0	0	t	0	$-t$	0
B, xy	t	0	0	0	0	0

TABLE III. The bond types of 24 bonds in one unit cell. Points and bonds are based on the notation in Fig. 3. "$\bar{i}$" is used for the points which are simply a translation by a basis vector from point "i."

Type x	Type y	Type z
(1,2)	(1,3)	(2,3)
(3,5)	(3,4)	(4,5)
$(\bar{5},7)$	$(\bar{5},6)$	(6,7)
(4,8)	(8,9)	(4,9)
$(8,\overline{11})$	$(7,\overline{11})$	(7,8)
$(\bar{1},\bar{6})$	$(\bar{6},12)$	$(\bar{1},12)$
(9,10)	$(\bar{2},9)$	$(\bar{2},10)$
(10,12)	(10,11)	(11,12)

$$J = \frac{2|\tilde{t}_{ij}^d|^2}{U_d}, \tag{46}$$

$$\mathbf{D}_{ij} = -\frac{4i}{U_d}(\mathbf{C}_{ij}^d \tilde{t}_{ji}^d - \tilde{t}_{ij}^d \mathbf{C}_{ji}^d), \tag{47}$$

$$\overleftrightarrow{\Gamma}_{ij} = \frac{4}{U_d}(\bar{\mathbf{C}}_{ij}^d \vec{\mathbf{C}}_{ji}^d + \hat{\mathbf{C}}_{ji}^d \vec{\mathbf{C}}_{ij}^d - 1(\mathbf{C}_{ij}^d \cdot \mathbf{C}_{ji}^d)). \tag{48}$$

F. Strong spin-orbit interaction

As discussed in Sec. I, in the strong spin-orbit limit, $\lambda \gg |\epsilon_{1,2} - \epsilon_3|$, one can obtain effective total angular momentum eigenstates with $j = 1/2$. Choosing Eq. (28), and rewriting the corresponding eigenstates in the canonical t_{2g} basis, Eq. (32) becomes

$$a_{i3\uparrow} = \frac{1}{\sqrt{3}}((-i)d_{i,xz\downarrow} + d_{i,yz\downarrow} + d_{i,xy\uparrow}), \tag{49}$$

$$a_{i3\downarrow} = \frac{1}{\sqrt{3}}((i)d_{i,xz\uparrow} + d_{i,yz\uparrow} - d_{i,xy\downarrow}), \tag{50}$$

in which we have expressed $a_{i3\uparrow}/a_{i3\downarrow}$ in terms of the t_{2g} annihilation operator to avoid the position dependence of the coefficients.

1. Superexchange through oxygen ions

The complicated expression of Eq. (42) requires simplification if we want to have a quantitative understanding of the exchange coupling. However, some information can be immediately obtained from Eq. (50), in particular that all $\tilde{t}_{i3,kn} = 0$, which makes J, $\mathbf{D}_{ij}$, and $\overleftrightarrow{\Gamma}_{ij}$ only the remaining terms with $\mathbf{C}_{i,kn}$. To simplify further, we need some explicit form for the transfer integrals $t_{jm,kn}$. Hence, we will make further approximation that the surrounding octahedra of Ir^{4+} are perfect so that we can apply the cubic symmetry to find out the nonvanishing transfer integrals and also the relation between

them, which is listed in Table II for Ir^{4+} A and B in Fig. 4. Deviations from these forms should presumably be small since the noncubic distortion is.

Based on the transfer integrals listed in Table II, we evaluate the exchange coupling constant J and $\overleftrightarrow{\Gamma}_{AB}$. For bond AB, collecting nonzero coupling constants (actually $J = 0$, $\mathbf{D}_{AB} = 0$), we obtain

$$\mathcal{H}_{AB} = -JS_A^x S_B^x + JS_A^y S_B^y + JS_A^z S_B^z, \tag{51}$$

with

$$J = \frac{4}{9}|t|^4(2g_{2p_x,5p_x} - g_{2p_x,2p_x} - g_{5p_x,5p_x}). \tag{52}$$

Since from Eq. (45) $g_{2p_x,5p_x} > g_{2p_x,2p_x}, g_{5p_x,5p_x}$, then $J > 0$. Thus we find ferromagnetic interaction between the x components and antiferromagnetic interactions between the y and z components along this link. This corresponds to the form in Eq. (1) of Sec. I, with $\epsilon_{ij}^y = \epsilon_{ij}^z = -\epsilon_{ij}^x = 1$ for this link.

Because all links are equivalent by point-group operations, we can deduce the exchange interactions of all other bonds by symmetry. The sites A and B correspond to point 4 and 8 in our notation in Fig. 3. The result is that the exchange interactions on each bond are ferromagnetic between one component, and antiferromagnetic between the other two. These principal components are always along x, y, or z. We will call a bond in which the x component is ferromagnetic a "type-x bond," and similarly for y and z. The type of each bond is listed in Table III. This Hamiltonian breaks spin rotational symmetry strongly. A simple rule can be used to characterize the Hamiltonian of a given bond: if bond (ij) is located in y-z plane, then the bond is type-x bond and has type-x exchange Hamiltonian; if it is located in x-z plane, then the bond is type-y bond and has type-y exchange Hamiltonian; if it is located in x-y plane, the bond is type-z bond and has type-z exchange Hamiltonian. As a result, the three bonds in every triangle (see Fig. 3) have different exchange Hamiltonian. The ground states of this Hamiltonian will be studied in Sec. IV.

2. Direct exchange

We consider two Ir atoms A and B, connected by a line along the $(0,1,-1)$ direction. There are two principle overlaps. The largest, whose magnitude we denote as t_1^d, is between the yz orbitals at each atom—this is a σ bond. A secondary overlap, of magnitude t_2^d, occurs between orbitals of the form xy-xz at each site, which corresponds to π bonding. All other overlaps are expected to be negligible or zero. This leads remarkably to

$$\tilde{t}_{j3,j'3}^d = (t_1^d + t_2^d)/3, \quad \mathbf{C}_{jj'} = 0. \tag{53}$$

The result appears isotropic despite the strong spin-orbit interactions. As a consequence, one obtains only Heisenberg exchange and $\mathbf{D}_{ij} = \overleftrightarrow{\Gamma} = 0$. It is remarkable that one finds apparent isotropy even though the spin itself contains a substantial orbital component. As seen from the superexchange calculation above, this is by no means guaranteed.

The first corrections to the strong spin-orbit limit are linear in the noncubic splittings, and produce corrections to the Heisenberg model. This occurs by a contribution to $\mathbf{C}_{jj'}$ of $\mathcal{O}(|\epsilon_3 - \epsilon_{1,2}|/\lambda)$. The leading spin-orbit corrections to the exchange Hamiltonian are then of the DM form, and constrained by symmetry according to considerations of Sec. III A.

G. Weak spin-orbit interaction

In this part, we are going to look at the weak spin-orbit interaction limit, $\lambda \ll |\epsilon_1 - \epsilon_2|, |\epsilon_2 - \epsilon_3|$. This is the regime which was often studied in literature.[13,16,17] Standard perturbation treatment can be applied, which yields

$$a_{jm\sigma} = d_{jm\sigma} + \frac{\lambda}{2} \sum_{m'\sigma'} \frac{\ell_{imm'} \cdot \boldsymbol{\sigma}_{\sigma\sigma'}}{\epsilon_m - \epsilon_{m'}} d_{jm'\sigma'} \tag{54}$$

with $\ell_{imm'}$ introduced previously in Eq. (24). Using this in Eq. (33) reproduces Eq. (31).

Keeping the exchange coupling constant to the linear order of $\frac{\lambda}{|\epsilon_{1,2}-\epsilon_3|}$, we can ignore $\overleftrightarrow{\Gamma}_{ij}$, as it is of $\mathcal{O}((\frac{\lambda}{|\epsilon_{1,2}-\epsilon_3|})^2)$ compared to J, thus we only need to evaluate J and $\mathbf{D}_{ij}$.

1. Superexchange through oxygen ions

Since all the bonds and sites are equivalent, we can take ij as bond BA in Fig. 4. We denote the unit directional vectors for D_1, D_2, and D_3 as $\mathbf{e}_1$, $\mathbf{e}_2$, and $\mathbf{e}_3$. Ignoring the small effect of lattice distortion on these vectors and taking the corresponding values for an ideal hyper-kagome lattice, we will get $\mathbf{e}_1 = \frac{1}{\sqrt{2}}(0,-1,1)$, $\mathbf{e}_2 = \frac{1}{\sqrt{3}}(-1,1,1)$, and $\mathbf{e}_3 = -\frac{1}{\sqrt{6}}(2,1,1)$. Making the same approximation as in previous section, we can evaluate the exchange coupling constants:

$$J = |t|^4 g_{2p_x,2p_x},$$

$$\mathbf{D}_1 = \mathbf{D}_{BA} \cdot \mathbf{e}_1 = \frac{\lambda}{\sqrt{2}} |t|^4 \left(\frac{g_{2p_x,2p_x}}{\epsilon_2 - \epsilon_3} - \frac{g_{5p_x,2p_x}}{\epsilon_1 - \epsilon_3} \right),$$

$$D_2 = \mathbf{D}_{BA} \cdot \mathbf{e}_2 = \frac{2\lambda}{\sqrt{3}} |t|^4 \frac{g_{5p_x,2p_x}}{\epsilon_1 - \epsilon_3},$$

$$D_3 = \mathbf{D}_{BA} \cdot \mathbf{e}_3 = -\frac{\lambda}{\sqrt{6}} |t|^4 \left(\frac{3g_{2p_x,2p_x}}{\epsilon_2 - \epsilon_3} - \frac{g_{5p_x,2p_x}}{\epsilon_1 - \epsilon_3} \right). \tag{55}$$

The three DM components we obtained in Eq. (55) are not independent from each other. That's because we render some symmetry to the system by the transfer integrals. Hence, we will still consider all three components to be independent. As discussed in Sec. III B, $\epsilon_3 > \epsilon_2 > \epsilon_1$. Additionally, we have $g_{kn,k'n'} > 0$ then we can confer from Eq. (55) that $J > 0$, $D_2 < 0$. D_3 is probably positive due to a factor of 3 in front of $g_{2p_x,2p_x}$ and the smaller denominator of the positive term than the negative term, and $|D_1|$ is probably small compared to $|D_2|$ due to the cancellation of positive and negative terms.

Using Eq. (55) and ignoring its specific expression, we may estimate the strength of DM interactions crudely. Then, we estimate crudely

$$|D_i|/J \approx \lambda/|\epsilon_{1,2} - \epsilon_3| \tag{56}$$

since we assume $\lambda \ll |\epsilon_{1,2} - \epsilon_3|$; otherwise the perturbative treatment does not hold. We estimate the spin-orbit coupling $\lambda \approx 0.4$ eV, taken from Refs. 20 and 21 (although the reference is not directly relevant to Na$_4$Ir$_3$O$_8$, we can use their spin-orbit coupling as an approximation). The splitting of the t_{2g} states due to the noncubic environment, which determines $\epsilon_{1,2} - \epsilon_3$, is difficult to estimate. As mentioned in Ref. 22, the $e_g - t_{2g}$ splitting for $[\mathrm{Ir(NH_3)_6}]^{3+}$ is about 5 eV. However, if we seek a *lower* bound on $|D_i|$ we can make do with what is probably an overestimate of this splitting. Taking $|\epsilon_{1,2} - \epsilon_3| \sim 5-10$ eV is surely in that category, and we therefore find $|D_i|/J \gtrsim 0.04-0.1$.

2. Direct exchange

One can similarly evaluate the induced DM terms at first order in the spin-orbit coupling in the case of direct exchange. One again obtains a $\mathbf{D}$ vector consistent with the symmetry considerations in Sec. III A.

IV. CLASSICAL GROUND STATES OF THE STRONG EXCHANGE ANISOTROPY HAMILTONIAN

In this section, we will consider the ground states of the strongly anisotropic Hamiltonian, Eq. (1), obtained in the strong spin-orbit limit from the Ir-O-Ir superexchange mechanism.

Take the triangle $\Delta 123$ in Fig. 3 for example. Bond $(1,2)$ is of bond type x; bond $(1,3)$ is of bond type y; bond $(2,3)$ is of bond type z. Then for bond $(2,3)$, the Hamiltonian is

$$\mathcal{H}_{(2,3)} = J(S_2^x S_3^x + S_2^y S_3^y - S_2^z S_3^z). \tag{57}$$

Clearly $\mathcal{H}_{2,3}$ is minimized if

$$\mathbf{S}_2^z = \mathbf{S}_3^z, \tag{58}$$

$$\mathbf{S}_2^{x,y} = -\mathbf{S}_3^{x,y}. \tag{59}$$

In general, for each bond, the energy is minimized if the ferromagnetically interacting components of the two spins involved are parallel, and the antiferromagnetically interact-

TABLE IV. The basis vectors for the ground-state spin configurations of the strong spin-orbit Hamiltonian.

	V_1			V_2			V_3		
Ir^{4+}	S_x	S_y	S_z	S_x	S_y	S_z	S_x	S_y	S_z
1	−1	0	0	0	−1	0	0	0	1
2	−1	0	0	0	1	0	0	0	−1
3	1	0	0	0	−1	0	0	0	−1
4	−1	0	0	0	−1	0	0	0	1
5	1	0	0	0	1	0	0	0	1
6	−1	0	0	0	1	0	0	0	−1
7	1	0	0	0	−1	0	0	0	−1
8	−1	0	0	0	1	0	0	0	−1
9	1	0	0	0	1	0	0	0	1
10	1	0	0	0	−1	0	0	0	−1
11	−1	0	0	0	−1	0	0	0	1
12	1	0	0	0	1	0	0	0	1

ing components are antiparallel. We can search for *unfrustrated* ground states by demanding this on every bond. Fixing one spin, its neighbors are therefore determined, and from them further neighbors, etc. It is straightforward to verify that in this procedure *no contradictions are encountered* despite the presence of loops on the lattice. In this way all classical ground states are determined from the choice of a single initial spin. Thus the Hamiltonian is unfrustrated, and we have found its full set of classical ground states. Mathematically, we can write the full spin configuration as

$$\mathbf{S}_i = s^x V_{1,i} + s^y V_{2,i} + s^z V_{3,i}, \qquad (60)$$

where $\mathbf{s} = (s^x, s^y, s^z)$ is a unit vector, and $V_{a,i}$ is the vector V_a corresponding to the ith spin in Table IV. We see that the ground states are parametrized by two continuous parameters—the angles specifying the orientation of the initial spin, or that of $\mathbf{s}$. This is actually an accidental degeneracy since the system has only discrete space-group symmetries, but it is very small. Still, it should be reduced to a discrete degeneracy by perturbations such as quantum or thermal fluctuations, or additional interactions, which will select a subset of these states.

V. CLASSICAL GROUND STATES INDUCED BY DZYALOSHINSKII-MORIYA INTERACTIONS

A. Order due to second component only

In Sec. III, we found that the direction of the DM vector for a single bond is arbitrary, i.e., not determined from symmetry considerations, and not calculable from microscopic theory without a more detailed understanding of matrix elements than we have at present. A general solution for the ground state with such an arbitrary DM vector is quite difficult because different triangles in the hyper-kagome lattice are located in different planes. In this subsection, we will consider the special case in which the DM vector is normal to the triangular plane, i.e., $D_1 = D_3 = 0$ (see Fig. 3). This is a

helpful starting point for the more general case which we will address thereafter.

As in the case of the nearest-neighbor kagome antiferromagnet, a nonvanishing D_2 (here, by D_2 we mean the component of DM vector which is normal to the kagome plane) selects coplanar ground states with 120° spin orientations on each triangle.[13–15] These are the only configurations in which the Heisenberg interactions on a triangle are minimized (i.e., the total sum of spins on a triangle is zero) *and* the DM interaction is minimized at the same time. In the kagome lattice, however, the coplanar ground-state manifold is highly degenerate, since rotating the spins in a single hexagon about the normal axis of the kagome plane by arbitrary angle generates a new ground state from any other one. In contrast, for the hyper-kagome lattice, the noncoplanar nature of different triangles reduces the degeneracy to just a pair of Kramer's degenerate (reversed) states. One of them is drawn in Fig. 2; the other one is generated by reversing all the spin directions. The chirality of the hyper-kagome lattice makes this state a ground state *only* for $D_2 < 0$. With the other sign of D_2, the DM and Heisenberg interactions cannot be simultaneously satisfied. We will call these states uncanted "windmill" states—see Fig. 2.

To see that the uncanted windmill states are the only classical ground states, see Fig. 6. Starting from triangle ABC—denoted ΔABC—a nonvanishing D_2 component prefers a coplanar spin configuration, which requires that spin A, B, and C should lie in the ΔABC plane and at 120 angles as dictated by the Heisenberg interaction. The same applies to ΔCDE. However, ΔABC and ΔCDE are not in the same plane, which confines the spin orientation of site C to be aligned with the intersection line of ΔABC and ΔCDE. We apply this result to all spins, and the Heisenberg interaction will select two states, which simultaneously minimize the Dzyaloshinskii-Moriya (DM) interaction with $D_2 < 0$. The magnetic unit cell of the windmill state is the same as the chemical cell.

The result that $D_2 < 0$ completely removes the massive but accidental ground-state degeneracy of the hyper-kagome
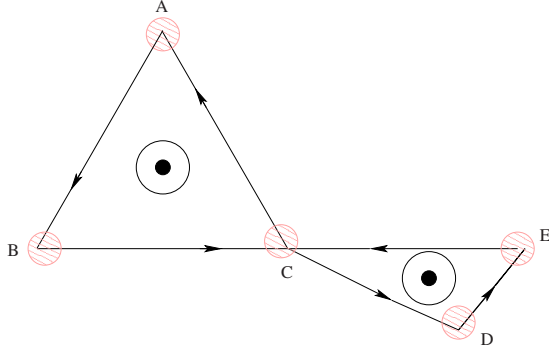
FIG. 6. (Color online) Illustration of spin direction at shared corner of two neighboring triangles. Black arrows indicate the DM interaction path. B, C, and E are in the same line.

is quite dramatic. A classical antiferromagnet with this interaction will clearly order at low temperature, and the drastic reduction in degeneracy suggests that even for a quantum system, the suppression of quantum fluctuations by D_2 may be large. Before turning to this, we continue with the analysis of classical ordering in the remainder of this section.

B. Magnetic representational analysis of space group

Representational analysis of the magnetic space group has proven to be a useful tool to extract information about low-temperature ordered phases using lattice symmetry.[23–26] The idea is to consider those types of magnetic order which can be reached by a continuous transition from the paramagnetic state, which has the full space-group symmetry. Although there is no *a priori* reason why the *ground-state* configuration need be of this type, this is a convenient way to generate candidate magnetically ordered states. In principle, one may iterate this procedure to generate lower temperature ordered states, generating all possible ordered phases.

The operators of the space group act on both the position of the magnetic ion and on the components of the spin vectors. The combination of these two results are described by the magnetic representation Γ. The magnetic representation for a particular site can be decomposed into contributions from the irreducible representations of the little group

$$\Gamma = \sum_{\mu} n_{\mu} \Gamma_{\mu}. \tag{61}$$

For Na₄Ir₃O₈, the space group is $P4_132$ (although it can also be $P4_332$, the results should be equivalent),[7] and the Ir⁴⁺ ions sit on the 12d. Here, we only focus the simplest case when the propagation vector $\vec{k}=(0,0,0)$. A program called "SARAH"[24] is used to do the decomposition of magnetic representation

$$\Gamma = 1\Gamma_1^{(1)} + 2\Gamma_2^{(1)} + 3\Gamma_3^{(2)} + 3\Gamma_4^{(3)} + 3\Gamma_5^{(3)}, \tag{62}$$
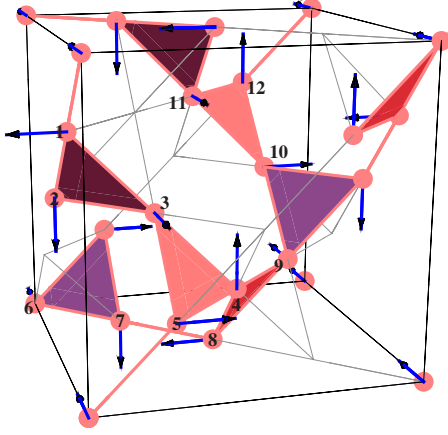
in which the superindex represents the dimension of the irreducible representations, and the subindex counts the irreducible representation.

Landau theory requires that only one representation can be involved in a critical transition, and so with this constraint there are only five possible magnetic structure for $\vec{k} = (0,0,0)$. Even within this decomposition and Landau theory constraints, for certain representations $(\Gamma_3, \Gamma_4, \Gamma_5)$, there still remain a lot of degrees of freedom because of the multiple basis elements in these three-dimensional representations. For simplicity, we only discuss one-dimensional representations Γ_1 and Γ_2. The basis vectors for these two representations calculated are given in Table V.

The physical interpretation of these representations is as follows. The basis vector ψ_1 is nothing but the C_2 rotation axis at every magnetic ion. The basis vector ψ_2 gives the spin directions of classical uncanted windmill state discussed above (see Fig. 2). The third basis vector ψ_3 (see Fig. 7) may be obtained as the axis which is normal to both C_2 axis and

TABLE V. The basis vectors of one-dimensional irreducible group representations of the space group $P4_132$ appearing in the magnetic representation with $\vec{k}=(0,0,0)$.

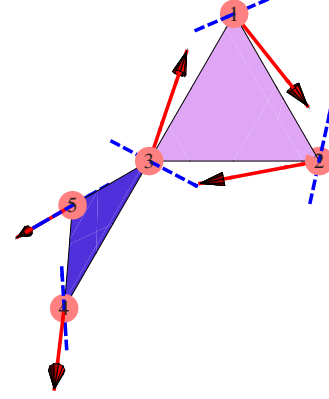| | $\Gamma_1^{(1)}$ | | | $\Gamma_2^{(1)}$ | | | | | |
| Basis vector | ψ_1 | | | ψ_2 | | | ψ_3 | | |
Ir⁴⁺	S_x	S_y	S_z	S_x	S_y	S_z	S_x	S_y	S_z
1	0	$\frac{1}{\sqrt{2}}$	$\frac{1}{\sqrt{2}}$	0	$\frac{1}{\sqrt{2}}$	$-\frac{1}{\sqrt{2}}$	-1	0	0
2	$\frac{1}{\sqrt{2}}$	$\frac{1}{\sqrt{2}}$	0	$\frac{1}{\sqrt{2}}$	$-\frac{1}{\sqrt{2}}$	0	0	0	-1
3	$\frac{1}{\sqrt{2}}$	0	$\frac{1}{\sqrt{2}}$	$-\frac{1}{\sqrt{2}}$	0	$\frac{1}{\sqrt{2}}$	0	-1	0
4	$-\frac{1}{\sqrt{2}}$	$\frac{1}{\sqrt{2}}$	0	$\frac{1}{\sqrt{2}}$	$\frac{1}{\sqrt{2}}$	0	0	0	1
5	0	$\frac{1}{\sqrt{2}}$	$-\frac{1}{\sqrt{2}}$	0	$-\frac{1}{\sqrt{2}}$	$-\frac{1}{\sqrt{2}}$	1	0	0
6	$-\frac{1}{\sqrt{2}}$	0	$\frac{1}{\sqrt{2}}$	$\frac{1}{\sqrt{2}}$	0	$\frac{1}{\sqrt{2}}$	0	1	0
7	$\frac{1}{\sqrt{2}}$	$\frac{1}{\sqrt{2}}$	0	$-\frac{1}{\sqrt{2}}$	$\frac{1}{\sqrt{2}}$	0	0	0	-1
8	0	$\frac{1}{\sqrt{2}}$	$\frac{1}{\sqrt{2}}$	0	$-\frac{1}{\sqrt{2}}$	$\frac{1}{\sqrt{2}}$	-1	0	0
9	$\frac{1}{\sqrt{2}}$	0	$-\frac{1}{\sqrt{2}}$	$-\frac{1}{\sqrt{2}}$	0	$-\frac{1}{\sqrt{2}}$	0	1	0
10	0	$-\frac{1}{\sqrt{2}}$	$\frac{1}{\sqrt{2}}$	0	$\frac{1}{\sqrt{2}}$	$\frac{1}{\sqrt{2}}$	1	0	0
11	$\frac{1}{\sqrt{2}}$	0	$\frac{1}{\sqrt{2}}$	$\frac{1}{\sqrt{2}}$	0	$-\frac{1}{\sqrt{2}}$	0	-1	0
12	$\frac{1}{\sqrt{2}}$	$-\frac{1}{\sqrt{2}}$	0	$-\frac{1}{\sqrt{2}}$	$-\frac{1}{\sqrt{2}}$	0	0	0	1

FIG. 7. (Color online) The basis vector ψ_3 in Table V.

FIG. 8. (Color online) The spin configuration of site 1, 2, 3, 4, and 5. The dashed blue lines are the canting axis of corresponding spin.

the spin direction in ψ_2 (see Fig. 2). Note that these three basis vectors at each site form an orthonormal basis for the spin coordinates.

Evidently Γ_2 is related to the DM interaction, at least to the D_2 component. But what about D_1 and D_3? Let us consider the following situation. Starting from an ordered ground state with $D_2 < 0$, we turn on an infinitesimal D_1 or D_3 component. The spin at site i can be written as

$$\mathbf{S}_i = \sqrt{1 - (a_i^1)^2 - (a_i^3)^2}\,\hat{e}_i^2 + a_i^1 \hat{e}_i^1 + a_i^3 \hat{e}_i^3, \tag{63}$$

where $\hat{e}_1$, $\hat{e}_2$, and $\hat{e}_3$ are simply the three orthogonal unit vectors given by basis ψ_1, ψ_2, and ψ_3, and a_i^1 and a_i^3 are small corrections to the ordered ground state due to the introduction of an infinitesimal D_1 (or D_3) component. We plug Eq. (63) into the Hamiltonian, and expand to the second order in a_i^1, a_i^3, and D_1 (or D_3). To linear order a_i^3 vanishes. Thus the ground-state spin configuration with negative D_2 and an infinitesimal D_1 or D_3 component is related to ψ_2 and ψ_3. The irreducible representation $\Gamma_2^{(1)}$ is relevant to the magnetic structure when the DM interaction is present.

Now, we proceed by assuming that the ground-state configuration ψ of the more general case, when D_1, D_2, and D_3 are all present in the system, is a linear superposition of basis vectors ψ_2 and ψ_3:

$$\mathbf{S}_i = \cos x\, \boldsymbol{\psi}_{2,i} + \sin x\, \boldsymbol{\psi}_{3,i}, \tag{64}$$

where $\boldsymbol{\psi}_{a,i}$ is the vector ψ_a corresponding to the ith spin in Table V. Evaluating Eq. (2) for spin configurations of this form gives

$$\mathcal{H}/N = 2(-3\sqrt{2}D_1 + 5\sqrt{3}D_2 - \sqrt{6}D_3 - 3J) + 2\sqrt{3}[(\sqrt{6}D_1 + D_2$$
$$+ \sqrt{2}D_3 - \sqrt{3}J)\cos(2x) - (\sqrt{3}D_1 - 3D_3)\sin(2x)], \tag{65}$$

where N is the number of unit cells in the lattice, not the number of spins (which is equal to $12N$). Minimizing the Hamiltonian with respect to x, we can find the canting angle x is given by

$$\cos(2x) = -\frac{-\sqrt{3}J + \sqrt{6}D_1 + D_2 + \sqrt{2}D_3}{W}, \tag{66}$$

$$\sin(2x) = \frac{\sqrt{3}D_1 - 3D_3}{W}, \tag{67}$$

where we have defined

$$W = \sqrt{(\sqrt{6}D_1 + D_2 + \sqrt{2}D_3 - \sqrt{3}J)^2 + 3(D_1 - \sqrt{3}D_3)^2} \tag{68}$$

for convenience.

Figure 8 is an example of this canted state when $D_1 = 0.1J$, $D_2 = -0.04J$, and $D_3 = 0$. We only plotted the spin configuration of $\Delta 123$ and $\Delta 345$ in Fig. 3. Because these states are obtained by smoothly introducing a ψ_3 component into the uncanted windmill states found in Sec. V, we will call this state a canted windmill state. The canted moment disappears not only when $D_1 = D_3 = 0$, but also for $D_1 = \sqrt{3}D_3$, at which point it degenerates into the uncanted windmill state. Regardless, it is also interesting to note that because D_1, $D_3 \ll J$, from Eq. (67) the canted moment is much smaller than the coplanar component, which indicates the dominance of the coplanar spin configurations. Similar features have been found in other studies.

In the above treatment, we have assumed the ansatz in Eq. (64), which is not guaranteed to find the global minimum energy state, and gives no guidance as to where this form of the ground state breaks down. In next section, we will consider this question from a different point of view.

C. Mean-field spherical model

In this subsection we approach the general problem of finding classical ground states of the Hamiltonian from a different point of view, which allows us to determine approximately when the $\mathbf{k} = (0,0,0)$ states of the previous subsection are (classical) ground states, and what the nature of the ground states otherwise are. The problem is difficult because in addition to minimizing $\mathcal{H}$, which is quadratic in spins, we must also satisfy constraints that each spin have fixed magnitude $|\mathbf{S}_i| = 1$. The large number (equal to the number of spins) of these constraints makes what otherwise would be a simple quadratic minimization problem difficult. Here we replace these many constraints by a single one,

$$\sum_i |\mathbf{S}_i|^2 = 12N, \qquad (69)$$

where as elsewhere in the text, we define N as the number of unit cells for convenience. This is the "spherical model," and is exactly soluble at both zero and nonzero temperature. At zero temperature, the spherical approximation *must* give a lower bound to the true ground-state energy since minimization is conducted with less constraints than in the physical spin model. Because of this observation, this approach can indeed often be used to construct physical ground states. This "Luttinger-Tisza" method[27–29] consists of finding a subset of ground states of the spherical model which respects the spin normalization constraints of the physical problem. Any such states must be ground states of the full Hamiltonian. Moreover, when such states exist, they exhaust the full set of physical ground states. However, it is not always possible to find any ground states of the spherical model which satisfy the normalization constraint. If not, it simply means that ground-state energy of the physical problem is strictly larger than that of the spherical model, and the Luttinger-Tisza method fails. Generally, the Luttinger-Tisza construction is less effective on lattices with a large number of sites in their basis. For the hyper-kagome lattice with a 12 site basis, our expectations should not be too high. Nevertheless, in some range of phase space, we will indeed find physical ground states from this approach. More generally, at nonzero temperature, the spherical model may be a useful approximation even when it fails to produce exact ground states at zero temperature.

Minimizing the quadratic Hamilton in Eq. (2) with the single global constraint in Eq. (69) is a standard problem, which is solved by finding the eigenvectors of the Hamiltonian matrix (coefficients of the quadratic form of spin components) with minimum eigenvalues. By translational invariance, the eigenfunctions have the Bloch form, i.e., are quasimomentum eigenstates. Hence it is useful to Fourier transform Eq. (2):

$$\mathcal{H} = N \sum_{\mathbf{k}} \sum_{i,j} \sum_{\nu,\mu} L_{\nu\mu}^{ij}(\mathbf{k}) Q_i^{\nu\dagger}(\mathbf{k}) Q_j^{\mu}(\mathbf{k}). \qquad (70)$$

Here

$$\mathbf{S}_i^\nu(\mathbf{R}_n) = \sum_k Q_i^\nu(\mathbf{k}) \exp(i\mathbf{k}\cdot\mathbf{R}_n), \qquad (71)$$

with ν, μ as indices of spin vector components, $\mathbf{R}_n$ is the position of unit cell, i and j are the sublattice index, and $L_{\nu\mu}^{ij}$ is the Fourier transformed Hamiltonian matrix in the Bloch representation (which is $12\times3=36$ dimensional because of the multiple basis sites and spin components). We need to minimize Eq. (70) subject to the soft constraint Eq. (72), which can be expressed as

$$\sum_{i=1}^{12} \sum_k \mathbf{Q}_i^\dagger(\mathbf{k}) \cdot \mathbf{Q}_i(\mathbf{k}) = 12. \qquad (72)$$

Minimization is equivalent to find the minimum eigenvalues (and corresponding eigenvectors) of $L_{\nu\mu}^{ij}(\mathbf{k})$. We did this numerically for every $\mathbf{k}$, and found the global minimum for
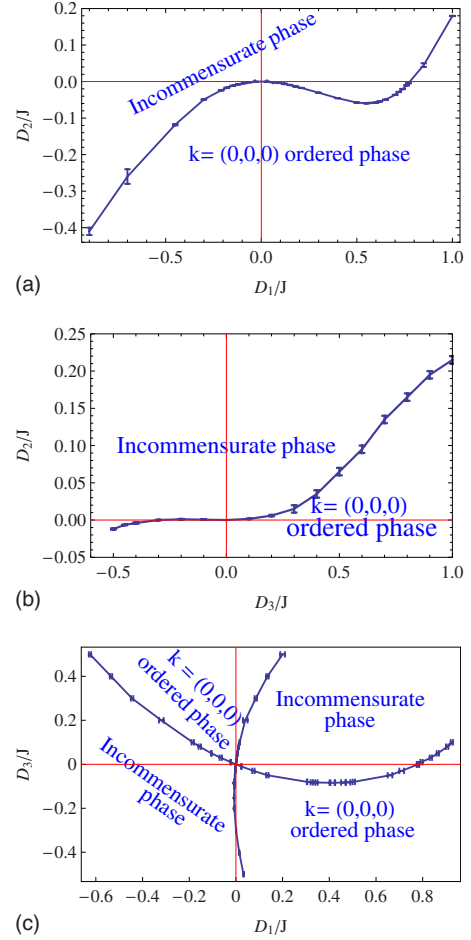

FIG. 9. (Color online) Phase diagram in D_1-D_2, D_2-D_3, and D_1-D_3 parameter spaces. The uninvolved DM vector component in each figure is set to be 0. The red reference lines (axes) are not phase boundary.

every (D_1, D_2), (D_2, D_3), and (D_1, D_3) pairs. With this approach, phase diagrams in D_1-D_2, D_2-D_3, and D_1-D_3 parameter spaces have been plotted in Fig. 9. In a wide region of the phase diagrams, the minimum eigenvalue is realized for $\mathbf{k}=(0,0,0)$. In this case, the corresponding eigenfunction *can* be chosen to satisfy the normalization constraint on every site, and so an exact ground state is found. This ordered state is in fact precisely the canted/uncanted windmill states we proposed in previous section. Thus in the regions for which $\mathbf{k}=(0,0,0)$ is indicated in the figures, this analysis proves that these windmill states are the exact global ground states. In a considerable large region of the parameter spaces, we get canted/uncanted "windmill" states.

In other broad regions of the phase diagram, the spherical model predicts ordered states with incommensurate wave vectors, i.e., in which $\mathbf{k}$ has irrational projection onto reciprocal lattice vectors. This is indicated simply as "incommensurate phase" in the figures. In most cases we have studied, the incommensurate wave vectors are located around $0.85(\pi, \pi, \pi)$ and its eight equivalent momenta $0.85(\pm\pi, \pm\pi, \pm\pi)$. However, in this region of the phase diagram, we are unable to construct a linear combination of eigenfunctions which satisfies the local constraint on the spin

magnitudes. Thus the incommensurate ground state of the spherical model does not immediately imply a corresponding ground state of the physical model. It is possible that the region of phase space occupied by the windmill states is actually expanded beyond what is shown here by this effect. Most likely, ground states with large unit cells or incommensurate order do exist in the physical model, but are more complex than those of the spherical approximation, and with somewhat higher energy. Even in the spherical model, we see that in the incommensurate region, while the DM interaction removes much of the frustration-induced degeneracy, the enlargement of the unit cell implies a larger residual ground-state degeneracy, and hence less effective removal of frustration than in the $\mathbf{k}=(0,0,0)$ regions.

VI. QUANTUM EFFECTS

A. Numerically constructed Bogoliubov transformation

In previous sections, the spins were treated classically and classical ground states were obtained. In this section, we discuss the quantum effect in the formalism of linear spin-wave theory. In certain regions of D_1-D_2, D_2-D_3 and D_1-D_3 parameter space, we have an ordered ground state. We will use the Holstein-Primakoff Boson approach to explore the quantum effects.[30] Now we express the spin operator as follows:

$$\mathbf{S}_i(\mathbf{R}_n) \cdot \hat{S}_i^{\mathrm{ord}} \simeq S - a_i^\dagger(\mathbf{R}_n) a_i(\mathbf{R}_n), \qquad (73)$$

$$\mathbf{S}_i(\mathbf{R}_n) \cdot \mathbf{e}_i^1 \simeq \frac{\sqrt{2S}}{2I} [a_i(\mathbf{R}_n) - a_i^\dagger(\mathbf{R}_n)], \qquad (74)$$

$$\mathbf{S}_i(\mathbf{R}_n) \cdot (\hat{S}_i^{\mathrm{ord}} \times \mathbf{e}_i^1) \simeq \frac{\sqrt{2S}}{2} [a_i(\mathbf{R}_n) + a_i^\dagger(\mathbf{R}_n)], \qquad (75)$$

where $\hat{S}_i^{\mathrm{ord}}$ is the unit vector along the spin order, $\mathbf{e}_i^1$ is the C_2 rotational axis at site i introduced in Sec. V B, $a_i^\dagger$ and a_i are the creation and annihilation operators of Holstein-Primakoff bosons at ith sublattice of unit cell at position $\mathbf{R}_n$, and we only keep the lowest order of $a_i^\dagger$ and a_i. Under this transformation, the Hamiltonian can be written as

$$\mathcal{H} = -\frac{S}{2} \sum_{i,j,\mathbf{k}} A_{ij}(\mathbf{k}) a_i^\dagger(\mathbf{k}) a_j(\mathbf{k}) + B_{ij}(\mathbf{k}) a_i^\dagger(\mathbf{k}) a_j^\dagger(-\mathbf{k}) + \mathrm{H.c.}, \qquad (76)$$

where we have dropped the constant term and high-order terms. Here, $A_{ij}(\mathbf{k})$ and $B_{ij}(\mathbf{k})$ are the coefficient matrix we end up with after doing Fourier's transform on the creation and annihilation operators. The Fourier transformations we used are

$$a_i^\dagger(\mathbf{R}_n) = \frac{1}{\sqrt{N}} \sum_{\mathbf{k}} a_i^\dagger \exp(i\mathbf{k} \cdot \mathbf{R}_n), \qquad (77)$$

$$a_i(\mathbf{R}_n) = \frac{1}{\sqrt{N}} \sum_{\mathbf{k}} a_i \exp(-i\mathbf{k} \cdot \mathbf{R}_n). \qquad (78)$$

Since there are 12 sublattices, using the analytical Bogoliubov transformation is hopeless to diagonalize the Hamil-

tonian. Here, we will use a numerically constructed Bogoliubov transformation (NCBT) introduced and discussed in detail by Refs. 31 and 32 to diagonalize Eq. (76), find the spin-wave energy gap and calculate the quantum corrections to the classical order. We write Eq. (76) as

$$\mathcal{H} = \sum_{\mathbf{k}} \mathbf{X}^\dagger(\mathbf{k}) \mathbf{H}(\mathbf{k}) \mathbf{X}(\mathbf{k}), \qquad (79)$$

where

$$\mathbf{X}(\mathbf{k}) = [a_1(\mathbf{k}) \ldots a_{12}(\mathbf{k}), a_1^\dagger(-\mathbf{k}) \ldots a_{12}^\dagger(-\mathbf{k})]^T, \qquad (80)$$

$$\mathbf{H}(\mathbf{k}) = -\frac{S}{2} \begin{pmatrix} A(\mathbf{k}) B(\mathbf{k}) \\ B^*(-\mathbf{k}) A^*(-\mathbf{k}) \end{pmatrix}, \qquad (81)$$

and the hermiticity of $\mathcal{H}$ requires that

$$A_{ij}(\mathbf{k}) = A_{ij}^*(\mathbf{k}), \qquad (82)$$

$$B_{ij}(\mathbf{k}) = B_{ji}(\mathbf{k}). \qquad (83)$$

We now introduce the canonical transformation

$$\mathbf{X}(\mathbf{k}) = \mathbf{Q}(\mathbf{k}) \mathbf{Y}(\mathbf{k}), \qquad (84)$$

where, $\mathbf{Y}(\mathbf{k})$ is given by

$$\mathbf{Y}(\mathbf{k}) = [b_1(\mathbf{k}) \ldots b_{12}(\mathbf{k}), b_1^\dagger(-\mathbf{k}) \ldots b_{12}^\dagger(-\mathbf{k})]^T, \qquad (85)$$

and satisfies

$$[b_i(\mathbf{k}), b_j^\dagger(\mathbf{k}')] = \delta_{ij} \delta_{\mathbf{k},\mathbf{k}'}. \qquad (86)$$

The transformation $\mathbf{Q}$ is required to diagonalize the Hamiltonian as

$$\mathbf{Q}^\dagger(\mathbf{k}) \mathbf{H}(\mathbf{k}) \mathbf{Q}(\mathbf{k}) = \Lambda(\mathbf{k}), \qquad (87)$$

where $\Lambda(\mathbf{k})$ is the diagonal eigenvalue matrix whose diagonal matrix elements are given by $[\epsilon_1(\mathbf{k}), \cdots, \epsilon_{12}(\mathbf{k}), \epsilon_1(-\mathbf{k}), \cdots, \epsilon_{12}(-\mathbf{k})]$. Using this transformation, the quantum correction to the classical spin polarization can be written as

$$dS = \frac{1}{12N} \sum_{n,i} \langle a_i^\dagger(\mathbf{R}_n) a_i(\mathbf{R}_n) \rangle$$

$$= \frac{1}{12N} \sum_{\mathbf{k},i} \langle a_i^\dagger(\mathbf{k}) a_i(\mathbf{k}) \rangle$$

$$= \frac{1}{24N} \sum_{\mathbf{k}} \langle \mathbf{X}^\dagger \mathbf{X} \rangle - \frac{1}{2}. \qquad (88)$$

At zero temperature, further making use of Eq. (84), Eq. (88) can be expressed as

$$dS = \frac{1}{2} \left\{ \frac{1}{12N} \sum_{\mathbf{k}} \sum_{i=1}^{12} [\mathbf{Q}^\dagger \mathbf{Q}]_{ii} - 1 \right\}. \qquad (89)$$

If we find the canonical transformation $\mathbf{Q}(\mathbf{k})$, the energy spectrum can also be obtained. With the energy spectrum, we can find the spin-wave energy gap, Δ. Some care must be taken as the numerical construction of the Bogoliubov transformation is effective only when there is an energy gap.
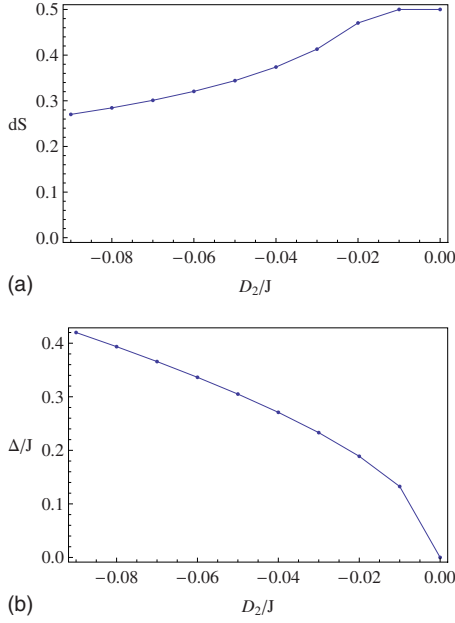
FIG. 10. (Color online) The dependence of quantum corrections and spin-wave gaps on the DM vector components. In the two figures, we set $D_1=D_3=0$ and vary D_2. $60\times60\times60$ momentum points have been used to generate the data. No change has been found in quantum corrections and gaps within computer resolution compared to $50\times50\times50$ momentum points.

B. Quantum corrections and spin-wave gaps

By the method described in last section, we carried out the numerical procedure described in Refs. 31 and 32. Taking spin $S=\frac{1}{2}$, we numerically construct the Bogoliubov transformation for every **k**, and find its contribution to zero-temperature quantum correction, dS, and energy levels at every **k** to extract the spin-wave gaps. The numerical results are plotted in Figs. 10–12 13. Corrections dS larger than 1/2 have been truncated to 1/2. In these figures, two components of the DM vector are kept constant while the third is varied. The ordered regions (the third varying DM vector component) of these figures can be found in Fig. 9.

In these figures, spin-wave gap is nonvanishing so our calculation is valid. It is easy to find the quantum behavior also resembles the classical one: the different DM vector components have different effects in quantum corrections, which is similar to the effect of DM vector components in favoring canted "windmill" state in Sec. V B. In the DM magnitude studied in these figures, the quantum corrections are pretty large. Even in the case when $D_2=-0.09J$ and $D_1=D_3=0$, the quantum correction is about 50%.

As a general rule, one observes that the quantum corrections decrease steadily as one goes deeper into the **k**=0 classically ordered region. If we crudely suppose that $dS>1/2$ is indicative of the destruction of order by quantum fluctuations, we may expect broad regions of quantum spin liquid states occurring in and near the incommensurate regions of the classical phase diagram. This range of DM vectors then may be possible candidates for application to Na$_4$Ir$_3$O$_8$.

C. Comparison with exact diagonalization

In order to partially confirm our results in last section, we performed numerical exact diagonalization for $S=1/2$
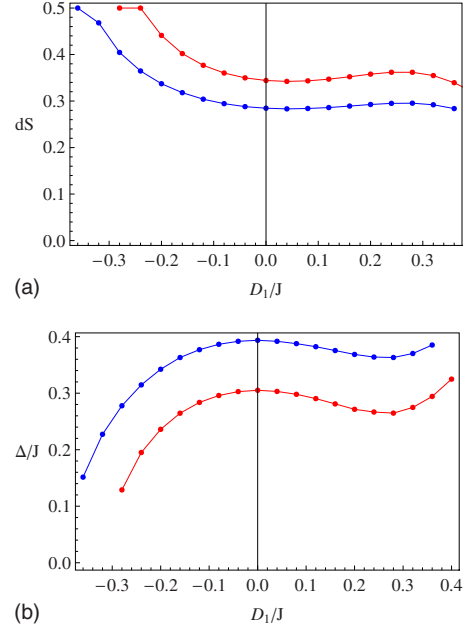

FIG. 11. (Color online) The dependence of quantum corrections and spin-wave gaps on the DM vector components. In the two figures, we set $D_3=0$ and vary D_1 with two fixed D_2 values [$D_2=-0.08J$ (in blue) and $D_2=-0.05J$ (in red)]. $16\times16\times16$ momentum points have been used to generate the data. No change has been found in quantum corrections and gaps within 1% compared to $10\times10\times10$ momentum points (same for Figs. 12 and 13).

spins.[33,34] We took six triangles with thirteen sites and used a Heisenberg model plus DM interaction with only $D_2\neq0$. We plot the resulting specific heat in Fig. 14. The gap in each
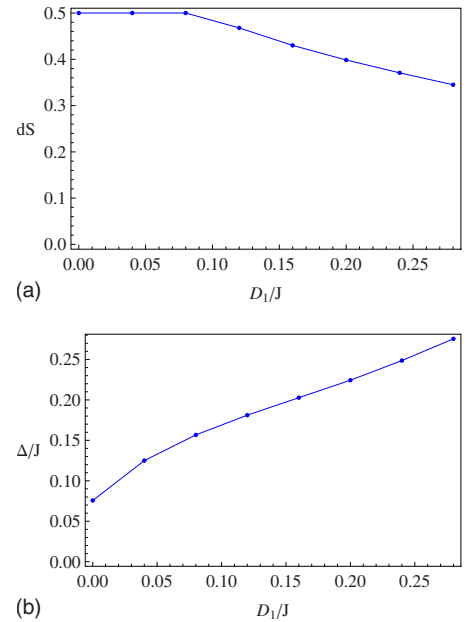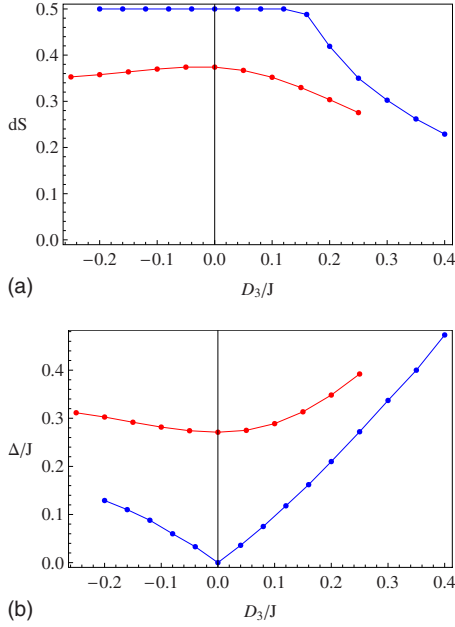

FIG. 12. (Color online) The dependence of quantum corrections and spin-wave gaps on the DM vector components. In the two figures, we set $D_2=0, D_3=-0.1$ and vary D_1. We also did the same thing with $D_2=0, D_3=0.1$, and varying D_1, and the quantum corrections always break the classical order completely.

FIG. 13. (Color online) The dependence of quantum corrections and spin-wave gaps on the DM vector components. In the two figures, we set $D_1=0$ and vary D_3 with two D_2 values [$D_2=0$ (in blue) and $D_2=-0.04J$ (in red)]. We also did the same thing with $D_2=0$, $D_3=0.1$, and varying D_1, and the quantum corrections always break the classical order completely.

case can be inferred from the plot by the temperature below which the specific heat becomes negligible. As we found in previous section, the more negative D_2 is, the greater the gap will be. At low temperatures in Fig. 14, the sequence of the curves agrees with what they should behave according to spin-wave gaps in Fig. 10.

Similarly, we also look at the case when only D_3 component is present by taking $D_3=\pm 0.10J$, $\pm 0.25J$. According to Fig. 13, the spin-wave gaps of $D_3=\pm 0.10J$ are close to each other, and the spin-wave gaps of $D_3=\pm 0.25J$ are also close to each other, but much larger than the previous cases. In Fig. 15, we see that both curves of $D_3=\pm 0.10J$ and $D_3=\pm 0.25J$ nearly overlap at low temperatures, and their sequence agrees with the magnitudes of the spin-wave gaps.
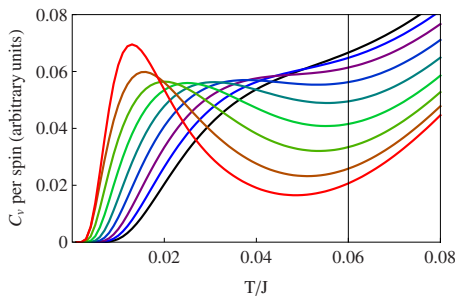

FIG. 14. (Color online) The specific heat of six triangles with negative D_2 component DM interaction. Along the thin vertical line, from top to bottom D_2 value of each curve increases from $-0.09J$ to $-0.01J$ with a step $0.01J$.
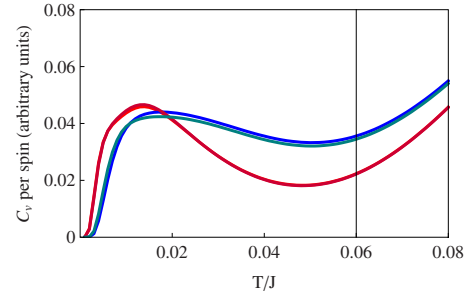

FIG. 15. (Color online) The specific heat of six triangles with D_3 component DM interaction. Along the thin vertical line, the upper curves have $|D_3|=0.25J$, the down curves have $|D_3|=0.10J$.

VII. DISCUSSION

In this paper we have studied the effect of spin-orbit interactions in the hyper-kagome lattice of $Na_4Ir_3O_8$. A crucial physical parameter is the strength of atomic spin-orbit coupling relative to noncubic crystal field splittings. In the strong spin-orbit limit, Ir-O-Ir superexchange produces highly anisotropic effective spin interactions, with 2/3 antiferromagnetic and 1/3 *ferromagnetic* couplings between spin components. This Hamiltonian turns out to be *unfrustrated*, and has a small set of classical ground states. We speculated that even the $S=1/2$ quantum model is likely ordered with a substantial critical temperature, inconsistent with experiments on $Na_4Ir_3O_8$.

By contrast, strong spin-orbit interactions and direct Ir-Ir exchange, or weak spin-orbit interactions all induce a Heisenberg-like Hamiltonian with a small correction of the form of a DM term. The orientation of the DM vector, which is not determined by symmetry or our microscopic considerations, determines the extent to which the frustration of the Heisenberg model is relieved. In one region of phase space, frustration is fully relieved, and the DM interaction stabilizes a magnetically ordered "windmill" state, with nearly but generically not quite coplanar moments. Quantum fluctuations, which we assessed by spin-wave theory, are sufficiently suppressed that we may expect this order to persist even for spin-1/2 spins (as in $Na_4Ir_3O_8$) in part of this region. In the remainder of phase space, the frustration is not fully removed, and the classical ground states break the lattice periodicity and may be incommensurate. We argued that in this regime, the classical ordering is fragile and may be destroyed by quantum fluctuations for $S=1/2$ spins.

A. Relation to previous work

Two theoretical papers[9,10] have discussed $Na_4Ir_3O_8$ prior to our own, as mentioned in Sec. I. Both start with the assumption of a simple nearest-neighbor Heisenberg model description. As we have repeatedly emphasized, the even approximate validity of a Heisenberg description is far from obvious due to strong spin-orbit coupling in Ir. One outcome of the present study is a mechanism by which an approximate Heisenberg form *is* obtained, from direct Ir-Ir exchange, despite strong spin-orbit interactions. This may be viewed as a partial *a postiori* justification for the starting

point of Refs. 9 and 10. Furthermore, the inclusion of non-negligible spin-orbit interactions is crucial to resolving the problem of the large experimental Wilson ratio, which we argued cannot be understood within *any* theory starting from a pure Heisenberg model.

Let us now comment upon the conclusions of these two works. In Ref. 9, the authors treated the spin as a classical $O(N)$ spin. By a large-N mean-field theory and classical Monte Carlo simulation, they found that the classical ground states are highly degenerate and a nematic order emerges at *very* low temperatures in the Heisenberg model ($N=3$). Because of the classical approximation, it is difficult to gauge the applicability of these results to the $S=1/2$ Heisenberg model, and the very-low-temperature results are probably irrelevant to the latter case. We view this paper as a point in favor of the notion that by itself the pure Heisenberg model has no strong tendency to favor any obvious ordered state. In the present article, since we have argued for the importance of modifications to the Heisenberg model, we have had to reconsider the ordering tendencies. Fortunately, there is a regime of DM interactions which do not appear to strongly remove the frustration.

In Ref. 10, the authors presented a large-N Sp(N) method and studied both the semiclassical spin and quantum spin regimes. In the semiclassical limit, they predicted that an unusual $\vec{k}=(0,0,0)$ coplanar magnetically ordered ground state is stabilized with no local "weather vane" modes. While in the quantum limit, a gapped topological Z_2 spin liquid emerges. Clearly, the semiclassical result is at odds with experiment, which is probably not surprising for $S=1/2$. Unfortunately, the Z_2 spin liquid also seems unsatisfactory in several respects. It is a fully gapped state, and so is inconsistent with the power-law specific heat seen in experiment. Moreover, any Z_2 spin liquid state in three dimensions is known to be separated by a *nonzero-temperature phase transition* from the paramagnetic high-temperature phase. This transition is expected to be of (inverted) Ising type, and as such have very clear signatures in thermodynamics, such as a diverging specific heat. No such (extremely exotic) transition is observed in experiments. Our own paper does not directly address the quantum ground state of Na$_4$Ir$_3$O$_8$. Rather, we have shown that strong quantum fluctuations are probably important even with substantial DM interactions (by showing that the spin-wave theory yields large corrections in the presumed physically relevant regime). The role of DM interactions in a fully quantum theory for Na$_4$Ir$_3$O$_8$ is an important and difficult problem for the future. As a first step, in the next subsection, we discuss a scaling theory of the susceptibility in this context.

B. Zero-temperature susceptibility in quantum spin liquids

Part of the motivation of the present study was the observation in Na$_4$Ir$_3$O$_8$ that the susceptibility χ tends to a constant at low temperature, despite the approximately quadratic decrease of specific heat. We argued that this combination, which implies a diverging Wilson ratio as $T \to 0$, is likely an indication of spin-orbit interactions. Indeed, on general grounds, a constant zero-temperature susceptibility is ex-

pected when SU(2) spin-rotation symmetry is broken. The situation of weak DM interaction is quite common in frustrated magnets, and may allow this behavior quite broadly. Therefore it is interesting to consider more generally how this occurs in the presence of weak DM coupling. We have not so far addressed the *magnitude* of this zero-temperature susceptibility.

Presuming the DM interaction to be relatively weak, the magnitude of χ should be understood in terms of the correlations the spins would have in the underlying system without DM. Various SU(2) invariant phases lead to rather different behaviors. Generally speaking, one expects the most suppressed χ for systems with the least low-energy spin fluctuations in the absence of DM. Probably the most extreme example is a valence bond solid (VBS) or dimer state, in which the eigenstates can be approximated by those of a single partition of the sites into pairs of spins which are coupled to each other only within the pairs. Such a VBS phase has a gap of order J to all excitations, including the elementary triplets. A simple calculation by second-order perturbation theory of the susceptibility shows that it is indeed nonzero, and of order

$$\chi_{\text{VBS}}(T=0) \sim \frac{D^2}{J^3}. \tag{90}$$

One may also estimate the magnitude of χ for various phenomenological gapless spin liquid ground states perturbed by Dzyaloshinskii-Moriya (DM). The general arguments follow scaling theory. We presume the gapless spin liquid is a critical phase in the renormalization group sense, described by a scale invariant field theory. Introduction of DM interactions breaks SU(2) symmetry, and allows operators $\mathcal{O}_\alpha$ breaking SU(2) to be added to the effective action/Hamiltonian. Generically, these appear with coefficients proportional to D. In the simplest situation, there is a single such operator $\mathcal{O}_\Delta$ with the smallest scaling dimension Δ. In most cases of interest, we expect $\Delta < d+z$, where d is the spatial dimension and z is the dynamical critical exponent ($z=1$ is common). In this case, the presence of this operator in the Hamiltonian constitutes a *relevant* perturbation. Then, if the susceptibility at $D=0$ behaves as $\chi \sim T^\beta$, we expect

$$\chi_{\mu\nu}(D,T) \sim T^\beta f_{\mu\nu}(D/T^{\frac{d+z-\Delta}{z}}), \tag{91}$$

where μ, ν are spin components x, y, z. The operator $\mathcal{O}_\Delta$ is expected to break SU(2) down to some subgroup. This may contain either one or zero residual U(1) spin-rotation axes. The susceptibility normal to this axis, if it exists, is expected to be constant at low temperature. If no such axis exists, then the susceptibility will be constant in all directions. In either case, we must have

$$f_{\mu\nu}(X) \sim A_{\mu\nu} X^{\frac{\beta z}{d+z-\Delta}}, \quad \text{for} \quad |X| \gg 1. \tag{92}$$

Here $A_{\mu\nu}$ is a symmetric tensor with either two or three nonzero eigenvalues, in the cases with one or zero residual U(1) symmetries, respectively. One thereby obtains

$$\chi_{\mu\nu}(T=0) \sim |D|^{\frac{\beta z}{d+z-\Delta}} A_{\mu\nu}. \tag{93}$$

As an example, consider the 2d "Dirac" spin liquid with point nodes on the kagome lattice studied by Hermele *et al.*[35] There, the dominant operator indeed preserves a single residual U(1) symmetry. Its scaling dimension is estimated as $\Delta \approx 2 - 32/(8\pi^2) \approx 1.6$ (based on a calculation for a generalized model with large number, N_f, of flavors of fermions, evaluated for the physical case $N_f=4$). Taking $d=2$, $z=1$, $\beta =1$ as appropriate for this case, we find, restoring units

$$\chi_{\perp}(T=0) \sim \frac{\mu_B^2}{J} \left| \frac{D}{J} \right|^{0.7}. \tag{94}$$

Here $\chi_{\perp}$ is the susceptibility in the x-y plane perpendicular to the conserved U(1) spin axis. We see that the dependence on D is *sublinear*, making for a very large susceptibility even for rather small D/J.

It is noteworthy that the scaling prediction above should occur regardless of the other properties of the system in the presence of DM interaction. The relevance of $\mathcal{O}_{\Delta}$ at the spin liquid fixed point indeed implies that it drives the system into a different phase, which may not be a spin liquid at all. This is believed to be the case for the above Dirac spin liquid, for which the resulting state is expected to be magnetically ordered.[35]

C. Other possibilities

One may wonder whether the weak and strong spin-orbit limits are the only possibilities for $Na_4Ir_3O_8$, and whether they might be distinguished more directly. Probably the principal difference in the two cases is the *sign* of the g factor. In the weak spin-orbit limit, one has approximately $\mathbf{M} \approx -2\mu_B\mathbf{S}$, while in the strong case, we find $\mathbf{M} \approx +2\mu_B\mathbf{S}$. While these lead to identical Curie laws, they are physically distinct (note that one cannot reverse the sign of $\mathbf{S}$ and maintain its canonical commutation relations). It should be measurable in other experiments such as nuclear magnetic resonance. Microscopic reasoning gives no reason why the Ir^{4+} spins might not be in an intermediate situation between the two extreme limits. However, in this case one would expect a g factor in between these two values, i.e., with substantially reduced magnitude. A large deviation would seem to be inconsistent with the measured spin susceptibility.

This tends to support the notion that $Na_4Ir_3O_8$ is either in the strong or weak spin-orbit limit, and not in between. Given the incompatibility of the strongly anisotropic Ir-O-Ir superexchange Hamiltonian in the strong spin-orbit case with experiment, we are led to believe the weakly anisotropic Hamiltonian with DM interactions is most appropriate (we note that "weak anisotropy" still allows for $|D|/J \sim 0.1$, which would have strong effects on the low-energy physics). This, however, still leaves open the issue of weak versus strong spin-orbit interactions. Though susceptibility experiments do not distinguish the two cases, they are physically distinct, and could be discriminated by magnetic resonance methods, for instance. So far as we are aware, all prior measurements of Ir^{4+} ions capable of this distinction have been interpreted in terms of the strong spin-orbit scenario (see for example, Ref. 36). This fundamental physical question in $Na_4Ir_3O_8$ warrants further investigation.

Could there be another scenario? We cannot rule out the possibility that other interactions might play a role. Perhaps further neighbor exchange or spin-lattice coupling might be significant. These are important subjects for future theoretical studies.

[1] R. Moessner, Can. J. Phys. **79**, 1283 (2001).

[2] A. P. Ramirez, Annu. Rev. Mater. Sci. **24**, 453 (1994).

[3] M. Gvozdikova and M. Zhitomirsky, JETP Lett. **81**, 236 (2005).

[4] C. L. Henley, J. Appl. Phys. **61**, 3962 (1987).

[5] J. Villain, R. Bidaux, J. Carton, and R. Conte, J. Dev. Physiol. **41**, 1263 (1980).

[6] D. Bergman, J. Alicea, E. Gull, S. Trebst, and L. Balents, Nat. Phys. **3**, 487 (2007).

[7] Y. Okamoto, M. Nohara, H. Aruga-Katori, and H. Takagi, Phys. Rev. Lett. **99**, 137207 (2007).

[8] Y. Shimizu, K. Miyagawa, K. Kanoda, M. Maesato, and G. Saito, Phys. Rev. B **73**, 140407(R) (2006).

[9] J. Hopkinson, S. Isakov, H.-Y. Kee, and Y. B. Kim, Phys. Rev. Lett. **99**, 037201 (2007).

[10] M. J. Lawler, H.-Y. Kee, Y. B. Kim, and A. Vishwanath, Phys. Rev. Lett. **100**, 227201 (2008).

[11] M. Rigol and R. R. P. Singh, Phys. Rev. B **76**, 184403 (2007).

[12] A. Kolezhuk, S. Sachdev, R. R. Biswas, and P. Chen, Phys. Rev. B **74**, 165114 (2006).

[13] M. Elhajal, B. Canals, and C. Lacroix, Phys. Rev. B **66**, 014422 (2002).

[14] R. Ballou, B. Canals, M. Elhajal, C. Lacroix, and A. S. Wills, Phys. Status Solidi B **236**, 240 (2003).

[15] M. Elhajal, B. Canals, and C. Lacroix, Physica B (Amsterdam) **312-313**, 716 (2002).

[16] T. Moriya, Phys. Rev. **120**, 91 (1960).

[17] W. Koshibae, Y. Ohta, and S. Maekawa, Phys. Rev. B **47**, 3391 (1993).

[18] J. Kanamori, Prog. Theor. Phys. **30**, 275 (1963).

[19] J. Goodenough, Phys. Rev. **171**, 466 (1968).

[20] N. Vugman and S. Nogueira, Rev. Bras. Fis. **19**, 606 (1989).

[21] S. Morov, I. Carmichael, and G. Hug, *Handbook of Photochemistry* (Dekker, New York, 1993).

[22] See R. Murugavel, http://www.chem.iitb.ac.in/%7Ermv/ch102/

cft.pdf, p. 11.

[23] A. S. Wills, Phys. Rev. B **63**, 064430 (2001).

[24] A. Wills, Physica B (Amsterdam) **276-278**, 680 (2000).

[25] J. Dimmock, Phys. Rev. **130**, 1337 (1963).

[26] E. Bertaut, Acta Crystallogr., Sect. A: Cryst. Phys., Diffr., Theor. Gen. Crystallogr. **24**, 217 (1968).

[27] D. Lyons, T. Kaplan, K. Dwight, and N. Menyuk, Phys. Rev. **126**, 540 (1962).

[28] J. Luttinger and L. Tisza, Phys. Rev. **70**, 954 (1946).

[29] J. Luttinger, Phys. Rev. **81**, 1015 (1951).

[30] T. Holstein and H. Primakoff, Phys. Rev. **58**, 1098 (1940).

[31] A. D. Maestro and M. Gingras, J. Phys.: Condens. Matter **16**, 3339 (2004).

[32] A. D. Maestro, M.S. thesis, University of Waterloo, 2003.

[33] F. Alet *et al.*, ALPS Collaboration, J. Phys. Soc. Jpn. **74**, 30 (2005).

[34] F. Albuquerque *et al.*, ALPS Collaboration, J. Magn. Magn. Mater. **310**, 1187 (2007).

[35] M. Hermele, Y. Ran, P. A. Lee, and X.-G. Wen, Phys. Rev. B **77**, 224413 (2008).

[36] A. Raizman and J. T. Suss, Phys. Rev. B **22**, 1141 (1980).